

**ASSAY DEVELOPMENT FOR AND EVALUATION OF SPHINGOMYELINASE D
AND ASSOCIATED ACTIVITIES IN VENOMS FROM *LOXOSCELES RECLUSA* AND
KUKULCANIA HIBERNALIS AND IN ISOLATED SOIL BACTERIA**

A Thesis
Presented to
The Academic Faculty

By
Hannah Lachmayr

In Partial Fulfillment
of the Requirement of the Degree
Master of Science in Biology

Georgia Institute of Technology

August 2021

**ASSAY DEVELOPMENT FOR AND EVALUATION OF SPHINGOMYELINASE D
AND ASSOCIATED ACTIVITIES IN VENOMS FROM *LOXOSCELES RECLUSA* AND
KUKULCANIA HIBERNALIS AND IN ISOLATED SOIL BACTERIA**

Approved by

Alfred H. Merrill, Ph.D., Thesis Advisor
School of Biological Sciences
Georgia Institute of Technology

Konstantinos T. Konstantinidis, Ph.D.
School of Civil & Environmental Engineering
and School of Biological Sciences
Georgia Institute of Technology

Thomas DiChristina, Ph.D.
School of Biological Sciences
Georgia Institute of Technology

Janet K. Hatt, Ph.D.
School of Civil & Environmental Engineering
Georgia Institute of Technology

Date approved: July 30, 2021

ACKNOWLEDGEMENTS

I would first like to thank Dr. Merrill, without whom this project would not have been possible or nearly as successful. Dr. Merrill has given guidance on most aspects of this project as well as done all of the syntheses himself. I have learned so much from Dr. Merrill that I do not think I could ever quantify it. Most of what I have learned is through observation. A person to look up to and respect in the highest manner seems to often say the least. You simply observe their behavior, actions, and words and think, “I want to be like that. How can I emulate that?”

Dr. Konstantinidis has kindly allowed me to use his lab and carry out nearly all bacterial work in it. I am grateful to have such an enthusiastic collaborator.

I thank Dr. DiChristina for serving as a member on my committee.

Dr. Hatt worked closely with me to develop a method to isolate the bacteria from the soil. I am appreciative of her willingness to help me and to give me alternative ideas when I got unexpected results. I am thankful for all of the time that Dr. Hatt devoted to spending in lab with me to show me techniques and answer questions. Dr. Hatt made the libraries of the extracted isolate DNA.

Yiling Hu helped in the isolation of the soil bacteria. Her desire to learn was both motivational and inspiring to me, and I am grateful to have had her as a friend in the lab.

Blake Lindner has been instrumental in the bioinformatics aspect of this project. He has performed and explained nearly all bioinformatic analysis of the isolate genomes.

The entire Kostas lab has been so welcoming and kind to me; working in this atmosphere has lifted my spirits and always put a smile on my face. Thank you to Lizbeth Davila-Santiago, Gyuhyon Cha, Kumru Kocaman, and others with whom I did not directly interact.

I am grateful for Jiyao Yu’s willingness to go out of his way to help me in the lab.

I am thankful to my roommates Jo, Hannah, and Lopa for encouraging me, cheering me on, and making me laugh daily. I am also thankful to my parents, Margaret and Philip, and the rest of my family and friends who vehemently support me.

Though this thesis has my name as the author, it is not written by just me. This thesis would not be what it is without the guidance and support of others, in both my academic and personal lives. I am lucky to have had excellent guidance and support.

LIST OF TABLES

Table 1. 100X Trace Elements Solution	28
Table 2. BSA Dilutions and Final Concentrations.....	34
Table 3. Summarized Information from the MiGA Webserver for Each Isolate.....	60

LIST OF FIGURES

Figure 1. Degradation Pathways of SM/Biosynthesis of Cer(1,3)P.	5
Figure 2. TLC of C12-NBD-Sphingolipid Standards under UV Mineral Light.....	16
Figure 3. TLC of Incubations of <i>L. reclusa</i> and <i>K. hibernalis</i> Venom with NBD-SM under UV Mineral Light.....	22
Figure 4. Soil Bacteria Isolation Process.....	32
Figure 5. Isolate 6 Growth on M9 Agar Medium Containing Different Carbon Sources.....	37
Figure 6. Standard Curve of BSA	39
Figure 7. Protein Concentration of Isolate Growth in Media with Cer(1,3)P as the Sole Carbon Source.....	42
Figure 8. TLC of Isolates 6 and 7 Growth on C8-Ceramide(1,3)P over Time with Iodine Staining.....	43
Figure 9. Protein Concentration of Supernatants.....	45
Figure 10. TLC of Incubations of Isolates 6 and 7 with NBD-SM and NBD-Cer(1,3)P at 1 Hour and 24 Hours under UV Mineral Light.....	46
Figure 11. Workflow of the Bioinformatic Analysis of Isolate Genomes.....	54
Figure 12. Isolate 4 Sequencing Quality and Classification Using the MiGA Webserver.....	56
Figure 13. Isolate 5 Sequencing Quality and Classification Using the MiGA Webserver.....	57
Figure 14. Isolate 6 Sequencing Quality and Classification Using the MiGA Webserver.....	58
Figure 15. Isolate 7 Sequencing Quality and Classification Using the MiGA Webserver.....	59
Figure 16. Alignment of Isolate 4 Genome to an SMase C.....	61
Figure 17. Heatmap Summary of Metabolic Modules Found on Each Isolate Genome.....	62

LIST OF SYMBOLS AND ABBREVIATIONS

C12	Lauroyl
C24	Lignoceroyl
AAI	Average Amino Acid Identity
AMP	Adenosine monophosphate
ANI	Average Nucleotide Identity
BLAST	Basic Local Alignment Search Tool
CDase	Ceramidase
Cer	Ceramide
Cer(1,3)P	Ceramide 1,3-cyclic phosphate
Cer1P	Ceramide 1-phosphate
CERK	Ceramide kinase
DAG	Diacylglycerol
DCCD	N,N'-dicyclohexylcarbodiimide
DIPE	2-[(Propan-2-yl)oxy]propane
DMF	N,N-dimethylformamide
DMSO	Dimethylsulfoxide
DPBS	Dulbecco's phosphate-buffered saline
ELISA	Enzyme-linked immunosorbent assay
FA	Fatty acid
GSL	Glycosphingolipid
HEPES	2-[4-(2-hydroxyethyl)piperazin-1-yl]ethanesulfonic acid
HKD	HxKxxxxDx6GSxN motif
HPLC	High-performance liquid chromatography
Kb	Kilobase pairs
KEGG	Kyoto Encyclopedia of Genes and Genomes
LPA	Lysophosphatidic acid
LPC	Lysophosphatidylcholine
Lyso SM	Sphingosylphosphorylcholine
MeOH	Methanol
MiGA	Microbial Genomes Atlas
MS	Mass spectrometry
MW	Molecular weight
NBD	Nitrobenzoxadiazole
NCBI	National Center for Biotechnology Information
NHS	N-Hydroxysuccinimide
PA	Phosphatidic acid
PAP	Purple-acid phosphatase family
PC	Phosphatidylcholine
PLase	Phospholipase
PLC	Phospholipase C

PlcH	Hemolytic phospholipase C
PLD	Phospholipase D
R _f	Retention factor
scPLD	<i>Streptomyces chromofuscus</i> phospholipase D
SM	Sphingomyelin
SMase C	Sphingomyelinase C
SMase D	Sphingomyelinase D
Sph	Sphingosine
Sph1P	Sphingosine 1-phosphate
TLC	Thin-layer chromatography
TopFluor	Dipyrrrometheneboron difluoride
UV	Ultraviolet

SUMMARY

Since a sphingomyelinase D (SMase D) enzyme is presumably the major agent in the necrosis and toxicity of the brown recluse spider venom by cleaving sphingomyelin (SM) to ceramide 1,3-cyclic phosphate (Cer(1,3)P), a rigorous but simple assay would aid in detecting the presence of this sphingomyelinase activity. Several Sicariidae spiders, such as the brown recluse spider *Loxosceles reclusa*, and some pathogenic bacteria contain phospholipase D (PLase D) enzymes that act on phospholipid substrates. PLases D that cleave SM to release the headgroup choline are also called SMases D. Although the lipid product of the *L. reclusa* SMase D was initially thought to be ceramide 1-phosphate (Cer1P), a transphosphatidylolation mechanism by *L. reclusa* SMase D has been shown to produce Cer(1,3)P. For this thesis, fluorescent nitrobenzoxadiazole (NBD) analogs of products that are known to be made by various types of SMases (i.e., ceramide, Cer1P and Cer(1,3)P) were synthesized and an elution solvent system was identified that fully resolves these compounds as well as the substrate NBD-SM using silica gel thin-layer chromatography plates. When venom from *L. reclusa* was assayed, the product was the expected NBD-labeled Cer(1,3)P. Venom from *Kukulcania hibernalis*, a spider that has been suggested to have SMase D but whose products have not yet been determined, was assayed as well and NBD-Cer(1,3)P was found to be produced. To explore additional biomedically relevant applications of these methodologies, such as to discover bacterial enzymes that can degrade sphingolipids, we attempted to isolate bacteria from the soil with enzymatic activity to degrade SM and/or cyclic Cer(1,3)P. Single isolates of soil microorganisms were selected based on their ability to grow on the restrictive carbon sources SM or Cer(1,3)P and then examined for their cleavage of NBD-SM and/or NBD-Cer(1,3)P. Of four candidate isolates, genome sequencing of two isolates was taxonomically assigned to *Klebsiella variicola*, a gram-negative bacterium and opportunistic

human pathogen. Unfortunately, in the timeframe of this thesis, the conditions to assay the degradatory enzymes were not found. In summary, this work has developed a facile assay for SMase D, characterized for the first time Cer(1,3)P as a breakdown product of the action of *K. hibernalis* venom on SM, and expanded the methodologies that are available for analysis of activities that produce and degrade Cer(1,3)P.

TABLE OF CONTENTS

ACKNOWLEDGEMENTS	iii
LIST OF TABLES	v
LIST OF FIGURES	vi
LIST OF SYMBOLS AND ABBREVIATIONS	vii
SUMMARY	ix
CHAPTER 1: INTRODUCTION	1
CHAPTER 2: TLC OPTIMIZATION	9
2.1 INTRODUCTION	9
2.2 MATERIALS AND METHODS.....	10
2.3 RESULTS	15
2.4 DISCUSSION.....	17
CHAPTER 3: VENOM ASSAYS	19
3.1 INTRODUCTION	19
3.2 MATERIALS AND METHODS.....	20
3.3 RESULTS	21
3.4 DISCUSSION.....	23
CHAPTER 4: ISOLATED BACTERIA ASSAY.....	25
4.1 INTRODUCTION	25
4.2 MATERIALS AND METHODS.....	26
4.3 RESULTS	37
4.4 DISCUSSION.....	48
CHAPTER 5: ISOLATED BACTERIA GENOMIC ANALYSIS	51
5.1 INTRODUCTION	51
5.2 MATERIALS AND METHODS.....	52
5.3 RESULTS	55
5.4 DISCUSSION.....	63
CHAPTER 6: SUMMARY OF FINDINGS AND SUGGESTIONS FOR FUTURE STUDIES	64
REFERENCES	66

CHAPTER 1: INTRODUCTION

Sphingolipids are one of the three main classes of lipids in cell membranes (sterols, sphingolipids, and glycerolipids). Prevalent in eukaryotes and some prokaryotes, sphingolipids had been widely known since their report by J.L.W. Thudichum in 1884.¹ He named the first compound "sphingosin" for its enigmatic properties, reminiscent of the Sphinx.

Sphingolipids are a broad category of molecules, which includes some that are highly hydrophobic and others that are amphipathic, having both hydrophilic and hydrophobic properties. The hydrophobic region of a sphingolipid consists of a sphingoid long-chain base (sphingosine) backbone. This backbone is often connected to a fatty acid via an amide bond (to make ceramide, Cer) and/or to head group moieties at the primary hydroxyl group, such as phosphocholine for sphingomyelin (SM).

In addition to structural functions, sphingolipids play important and complex roles in cell signaling. For example, Cer is a precursor to other signaling sphingolipids, such ceramide 1-phosphate (Cer1P), as well as sphingomyelins and glycosphingolipids. The more complex sphingolipids have a large hydrophilic head groups that function in receptor regulation and cell-cell and cell-matrix interactions; whereas ceramide has only a small hydrophilic region of two hydroxyl groups and tends to aggregate in membranes.

With more than 20 species of fatty acids and five sphingoid bases, modification of this basic sphingolipid structure can yield hundreds of different combinations of "ceramides."² Likewise, complex sphingolipids are highly diverse as phosphosphingolipids (sphingomyelins) and

glycosphingolipids (GSL) with hundreds of combinations of sugar(s) added as their headgroups. All being derived from ceramide(s), sphingomyelins and glycosphingolipids can have a wide range of sphingoid bases and acyl chains of different lengths that further contribute to the variety of sphingolipid structures. The diversity of sphingolipid structure and function is rooted in common catabolic and synthetic pathways. Sphingolipid metabolism is “an array of interconnected networks” that originates from a common entry point and ends at a common breakdown point.³

This thesis is focused specifically on sphingomyelins and some of their important degradation products. SM is produced by sphingomyelin synthases, which are evolutionarily similar to the lipid phosphate phosphatase family.⁴ Formed by transfer of the headgroup phosphocholine from phosphatidylcholine to ceramide, the products sphingomyelin and diacylglycerol (DAG) are thought to regulate cell fate.⁵ Catabolism of sphingomyelin by mammals leads to ceramide (from sphingomyelinases in the phospholipase C family), sphingosine (via ceramidases), and then a compound that is both an intermediate of degradation and involved in signaling, sphingosine-1-phosphate. Sphingosine is phosphorylated to sphingosine-1-phosphate by two sphingosine kinases. Ceramide is also found in mammals as ceramide 1-phosphates via its phosphorylated by ceramide kinase (CERK).

Defects in catabolism of sphingolipids cause a wide number of diseases—for example, Niemann-Pick disease from defective degradation of sphingomyelin. As noted earlier, the major pathway of SM breakdown is via sphingomyelinases C (SMases C) which produce phosphocholine and ceramide as shown in Figure 1. Sphingomyelinases are part of a broader category of enzymes

called phospholipases (PLases). Phospholipases cleave the headgroup of phospholipids and are known for many types of phospholipids (for example, phosphatidylcholine (PC) is cleaved to diacylglycerol and the choline phosphate head group by phospholipase C, PLC). The “D” family enzymes (phospholipase D, PLD) cleave the phosphate bond between the phosphate and the headgroup; therefore, cleavage of PC by phospholipase D yields phosphatidic acid (PA) and choline. In some cases, the phospholipases D can perform transphosphatidylation instead of cleavage—i.e., for the lipid phosphate product to be a phosphodiester with either an alternative hydroxyl compound (for example, an alcohol that has been added to the assay) or in some cases, a hydroxyl of the lipid itself, such as a cyclic-lysophosphatidic acid or ceramide 1,3-cyclic phosphate.

Phospholipases that cleave at the phosphate bond are known for both glycerophospholipids and phosphosphingolipids. Phospholipase D activity was initially described in plants^{6–10} and has since been found in prokaryotic, viral, and eukaryotic organisms. As of this writing, there are over 15,000 phospholipase D enzymes that have been entered in NCBI GenBank. Most enzymes with phospholipase D activity have a conserved HxKxxxxDx6GSxN motif (HKD) or a variation of this motif which is responsible for the catalytic mechanism.^{11–13} An enzyme can still have phospholipase D activity and lack a conserved HKD motif. Enzymes that lack a conserved HKD motif are not a part of the HKD superfamily but cleave phosphodiester bonds in a similar manner. The most well characterized non-HKD phospholipase is that from *Streptomyces chromofuscus* (scPLD).¹⁴ This enzyme is thought to be secreted from *S. chromofuscus* to scavenge for phosphate.¹⁴ scPLD employs a metal-coordinated reaction mechanism that is similar to that of the purple-acid phosphatase family (PAP),¹⁵ using an Fe³⁺ cation for the

catalyzed reaction mechanism and an Mn^{2+} cation for substrate binding. Even though scPLD can perform transphosphatidylation, it does so less effectively than HKD PLD enzymes.¹⁶

The venoms of some spiders contain a phospholipase D enzyme which attacks the prey's sphingolipids. The brown recluse spider, *Loxosceles reclusa*, and other *Loxosceles* species express phospholipase D-like enzymes that act on SM and have been called sphingomyelinases. The phospholipase D that is found in the venom from *Loxosceles* spiders is manganese-dependent and does not have a conserved HKD motif but releases choline and (it was long thought) generate ceramide 1-phosphate.^{17,18} The action of this sphingomyelinase D (SMase D) is shown in Figure 1. As the primary toxic component of *Loxosceles* spider venom, sphingomyelinase D is thought to be largely responsible for hemolysis and the dermonecrosis that is seen when a human is bitten by one of these spiders.¹⁹⁻²¹

Loxosceles phospholipases D targets both lysophosphatidylcholine (LPC) and sphingomyelin as substrates in mammalian cell membranes.²²⁻²⁴ Phospholipase D activity has been commonly detected by the release of choline from SM and subsequent formation of the presumed product ceramide 1-phosphate.^{20,24-27} The pathology of *Loxosceles* envenomation was thought to hinge upon the presence of Cer1P.^{27,28} However, ³¹P NMR spectroscopy and mass spectrometry have revealed that action of the *Loxosceles* phospholipase D on the substrate sphingomyelin actually yields the formation of a cyclic product (Figure 1).²⁹ This cyclic product is formed by intramolecular transphosphatidylation and named ceramide 1,3-cyclic phosphate (Cer(1,3)P).

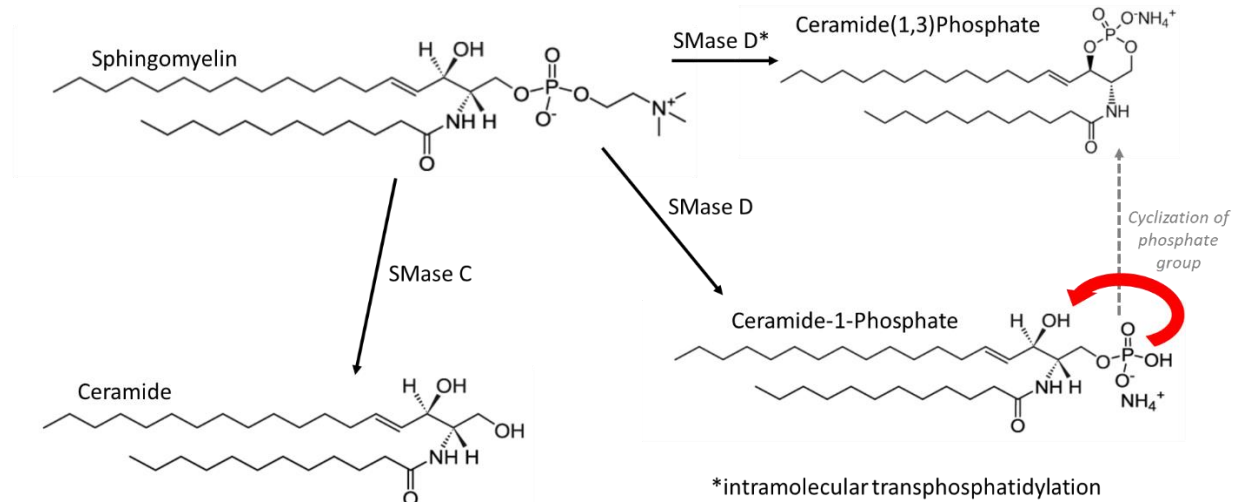


Figure 1. Degradation Pathways of SM/Biosynthesis of Cer(1,3)P. An SMase C cleaves the phosphocholine group of SM to yield ceramide. An SMase D cleaves just the choline group of SM to yield Cer1P or cyclizes the phosphate group to yield Cer(1,3)P.

It has been suggested that the formation of Cer(1,3)P by enzymatic activity of the venom contributes directly to the pathology of *Loxosceles* envenomation,²⁹ possibly by disrupting lipid bilayer morphology and integrity³⁰ and cell lysis from a change in membrane asymmetry.^{23,31,32} It can be envisioned, also, that Cer(1,3)P might play a role in cell signaling since it is a structural analog of the signaling sphingolipid Cer1P. Production of the cyclic phosphate might pose a long-term problem for mammals because it does not appear that there is an enzymatic activity in mammalian cells that cleaves this compound.³³

The venoms of a few other spiders, such as the *Kukulcania hibernalis*, have been suggested to have a SMase D, based on cross-reactivity of *K. hibernalis* venom to an antigenic assay for *L. reclusa* venom detection.^{34,35} In addition, there are occasionally reports of dermonecrosis as a side effect of *K. hibernalis* spider bites,³⁶ and dermonecrosis a classic characteristic of *L. reclusa*

envenomation in mammals. To date, there have been no published reports directly demonstrating SMase D activity in these other venoms; however, previous students in the Merrill laboratory found that incubation of *K. hibernalis* venom with fluorescently-tagged SM yields a product similar to that of an incubation of *L. reclusa* venom with fluorescently-tagged SM. At the time, this product was thought to be Cer1P and was not pursued further. With the finding that the *L. reclusa* enzyme produces Cer(1,3)P, it became interesting to determine if the *K. hibernalis* venom was actually producing that product, but a facile assay for this activity was not available.

Another reason that a facile assay for production of Cer(1,3)P from SM would be useful is that a wide range of organisms, including bacteria and fungi, are known to produce phospholipase Ds or candidates for this activity based on genetic homologies. The bacterial phospholipase D enzymes typically show more homology to plant phospholipases D, some bacterial phospholipases D appear to be more homologous to fungi and mammalian phospholipases D. *P. aeruginosa*'s harnessing of sphingolipids and subsequent infection have been the best studied of all bacteria.³⁷ Of the *Pseudomonas* strains identified in nature, about 30% express a *pldA* gene encoding for an HKD PLD.³⁸ The Gram-negative bacterium *Pseudomonas aeruginosa* is an opportunistic human pathogen that infects individuals with weak immune systems^{39,40} and is the main cause of mortality in patients with cystic fibrosis. Recombinant *Pseudomonas* PLD cleaves phosphatidylcholine to produce phosphatidic acid and performs transphosphatidylation in the presence of primary alcohols. Phospholipase D in *Pseudomonas* may or may not function as a virulence factor or be a part of homeostasis of the bacteria since phosphatidylcholine is in the inner and outer membrane leaflet of *Pseudomonas aeruginosa*.³⁸ In *pldA* deletion strains, long-term survival is decreased, but infectivity is unchanged. This gene was most likely acquired

from horizontal gene transfer from a higher organism, as Basic Local Alignment Search Tool – Nucleotide (BLASTN) of the National Center for Biotechnology Information (NCBI) database shows that the sequence for *pldA* is most homologous to mouse PLD2.¹¹ It has been suggested that a key way for bacteria like *P. aeruginosa* to hijack their hosts' cells is by manipulating membrane stability and lipid biogenesis, hijacking their immune response and sphingolipid balance in host cells.⁴¹

The aims of this thesis are fourfold. Aim one is to optimize a thin-layer chromatography (TLC) system for use in assaying sphingomyelinase D activity with fluorescent substrates. Once developed, it would be predicted to be useful in studying this activity in spider venoms and other organisms.

Aim two is to apply the assay to confirm the known sphingomyelinase D activity of *L. reclusa* venom and to, for the first time, characterize the activity of *K. hibernalis* venom.

Aim three is to begin to examine how bacteria utilize these sphingolipids. This was done by isolating environmental soil bacteria based on their ability to grow on a restrictive carbon source, SM and Cer(1,3)P.

Aim four is to genomically and taxonomically characterize these isolated bacteria from aim three.

It is hoped that these tools will be useful for a wide range of biochemical and biomedical studies, such as explorations of novel treatments for the injury caused by the SMase D of *L. reclusa* venom and other sources.

CHAPTER 2: TLC OPTIMIZATION

2.1 INTRODUCTION

The goal of these experiments was to optimize a thin-layer chromatography (TLC) system for use in assaying sphingomyelinase D activity with fluorescent substrates. This required the identification of a solvent system that would separate the fluorescently-tagged compounds of interest: Cer, SM, FA, Cer1P, and Cer(1,3)P. Due to the importance of Cer(1,3)P as the product of the venom SMase D, the conditions were selected to provide an unambiguous discrimination of this from the products of other categories of SMases (i.e., Cer for SMase C and Cer1P from SMase D's that catalyze hydrolysis rather than transphosphorylation reactions). It was also considered desirable to be able to prepare a “cocktail” mixture of these standards to run in a single lane of a TLC plate.

2.2 MATERIALS AND METHODS

Sources of Reagents

Fluorescent lipid analogs (C12-NBD-Cer, catalog # 810211; C11-TopFluor-Cer1P, catalog # 810270; and C12-NBD-SM, catalog # 810219) were obtained from Avanti Polar Lipids (Alabaster, AL). The C12-NBD-fatty acid was obtained from Molecular Probes (Eugene, OR). The HPLC-grade organic solvents (chloroform, #EM-CX1050 and methanol, #EM-MX0475) were obtained from VWR (West Chester, PA); ACS-grade acetic acid (#A38C-212) was obtained from Fisher Scientific (Waltham, MA); and all other solvents were analytical grade. N,N'-dicyclohexylcarbodiimide and iodine were from Sigma-Aldrich (St. Louis, MO). The thin-layer chromatography plastic sheets (Silica gel 60, # 105719) were from EM Science (Darmstadt, Germany).

The SMase D from *L. reclusa* venom was obtained via Chuck Kristensen at Spider Pharm (Yarnell, AZ).

Syntheses

C12-NBD-Cer1P was synthesized from S1P by modifying the method of Futerman and Pagano,⁴² for synthesis of NBD-Cer from sphingosine as follows: To a 13 x 100 mm screw-capped borosilicate glass test tube with Teflon-lined cap was added ~ 10 μ mol of C12-NBD-FA (MW 378 = 3.8 mg) dissolved in 0.1 mL of anhydrous DMSO (a gift from Dr. Christoph Fahrni at Georgia Tech), then ~ 10 μ mol of NHS (MW 115 = 1.2 mg) and ~ 15 μ mol of DCCD (MW 206 = 3.2 mg) were added in 0.4 mL of anhydrous DMSO. The test tube was purged with N₂ gas, tightly capped and sealed with parafilm, then wrapped with aluminum foil to react with rocking for 2 days at room temperature in the dark. The production of the NBD-aminohexanoic acid N-

hydroxyl succinimidyl ester was established by TLC using silica plates and CHCl_3 :MeOH (9:1, v/v) as the developing solvent (the R_f of the NHS ester was ~ 0.9 versus the free acid at ~ 0.5). To the test tube was added 10 μmol of S1P (4 mg) that was mostly dissolved in 2 mL of DMSO plus 20 μmol of DIPE (2.7 mg), and the test tube was purged with N_2 , sealed, covered with aluminum foil and rocked for 3 days at room temperature in the dark. Examination of the products by TLC indicated that the fluorescence was about equally distributed among unreacted NBD-fatty acid, C12-NBD-Cer1P, and C12-NBD-Cer1,3P (the latter was apparently formed from excess DCCD).

The products were extracted by adding chloroform and water to have two phases, with most of the color in the chloroform layer and interface. The upper layer was reextracted with a small volume of chloroform which was added to the first extract. The pooled extracts were mostly dried under N_2 , (a residue of DMSO remained), then redissolved by addition of chloroform for purification by column chromatography as described below.

C12-NBD-Cer(1,3)P was obtained as a byproduct of the synthesis of C12-NBD-Cer1P from S1P because the DCCD used in the amide coupling caused substantial cyclization, as mentioned above, and purified by column chromatography as described below. The identity was established by co-elution with other synthetic Cer(1,3)P by thin-layer-chromatography on silica gel 60 plates developed with CHCl_3 :MeOH:2N NH_4OH (60:25:2, v/v/v) as the developing solvent.

After brown recluse spider venom was confirmed to make the 1,3-cyclic phosphate (see results), the venom could be used to synthesize C12-NBD-Cer(1,3)P from C12-NBD-SM. For this method, 1 mg of C12-NBD-SM was suspended in 0.2 mL of 50 mM HEPES buffer (pH 7.5) and incubated with 10 μL of a 1:10 dilution of brown recluse venom for an hour at room

temperature, then examined by TLC. Since all of the C12-NBD-SM had been converted to C12-NBD-Cer(1,3)P, the reaction mixture was dried under N₂, then redissolved, and the product was purified using a small silica column.

Purification of NBD-C12-Cer1P by Silica Gel Column Chromatography

The NBD-C12-Cer1P was separated from most of the other components of the reaction mixture by silica gel column chromatography with elution by chloroform and increasing proportions of methanol. The silica gel (Unisil, Supelco) was suspended in chloroform and added rapidly to a small glass column (ca. 1 cm in width x 6 cm in height) with a glass frit until the settled bed of silica gel was approximately 2/3 the volume of the column in height. Then, the column was washed with several mL of chloroform and drained until the solvent reached the top of the column. Examination of the eluate showed that silica was not leaking through the frit, so without allowing the solvent to run dry at the top of the column, the reaction products (dissolved in ~ 1.5 mL of chloroform and sonicated for 10 minutes) were loaded to the column and washed with several mL of additional chloroform. All but a small amount of the reaction products was added to the column; this small amount was reserved for visualization on TLC. Fractions of approximately 10 mL each were collected in glass test tubes (16 x 100 mm) from the time that the reaction mixture was added to the column. In each step, 20 mL of the following solvent mixtures (chloroform with increasing % methanol) were added to the top of the column (with care not to disturb the silica) and the eluate from each collected into a test tube; the percentages of methanol were 0%, 1%, 5%, 10%, 17.5%, 25%, 35%, and 50%. The solvents were evaporated down in the methanol percentage of interest (25%) until about 1 mL remained in each test tube; the same was done for the few test tubes before and after the series.

Aliquots of each fraction were spotted onto TLC plates along with Cer1P and S1P standards. One lane was co-spotted with Cer1P and a concentrated eluant. The plate was run in a solvent of $\text{CHCl}_3:\text{MeOH}:\text{H}_2\text{O}$, 60:30:2, v/v/v. The fractions were visualized with UV mineral light (long wavelength), and the non-fluorescent Cer1P and S1P standards were visualized by iodine staining (as expected, the DCCD eluted in the early fractions from the column). The plates were also visualized in plain light to see the intensity of the yellow bands. The solvent from the fractions (10%, 25%, and 35%) that yielded greatest desired product (NBD-C12-Cer1P) were blown off with nitrogen and the residues were redissolved in 0.5 mL of $\text{CHCl}_3:\text{MeOH}$, 1:1, v/v. The redissolved fractions of the NBD-C12-Cer1P synthesis were run on TLC alongside standards and found to be pure. Minor modifications of this elution protocol could be used to purify other products of interest (such as Cer(1,3)P).

Creation of a “Cocktail” of Standards

The five fluorescent sphingolipids of interest: C12-NBD-Fatty Acid, C12-NBD-Ceramide, C12-NBD-Ceramide(1,3)P, TopFluor-C11-Ceramide 1-P, and C12-NBD-Sphingomyelin were suspended in ethanol and the concentrations estimated using the molar extinction coefficient for NBD of $\sim 25000 \text{ M}^{-1}\text{cm}^{-1}$ at 480 nm⁴³ and for TopFluor of $\sim 95000 \text{ M}^{-1}\text{cm}^{-1}$ at 495 nm,⁴⁴ using the Beer-Lambert law. The standards were mixed at approximately the same concentration to produce a single “cocktail” solution that could be run in one column of the TLC plate. The inclusion of TopFluor-C11-Ceramide 1-P in this cocktail will be explained in the “Discussion.”

TLC Optimization

The initial TLC conditions that were used had previously been reported to separate C6-NBD-Cer1P and C6-NBD-Cer(1,3)P,³³ which are more polar than the C12/C11 species. The two best

solvents for separation of C24-Cer1P and C24-Cer(1,3)P (and the corresponding C24-SM) were initially found to be CHCl₃:MeOH:H₂O:CH₃COOH (60:20:2:1, v/v/v/v) and CHCl₃:MeOH:H₂O (60:20:2, v/v/v),⁴⁵ however, Cer(1,3)P and Cer1P migrated relatively close to each other and these were important compounds to separate. Thus, alternative solvents were tested to achieve better separation by varying not only the original components (using various combinations of two or more of the following: chloroform, methanol, acetic acid and water), but also, substituting 2N ammonium hydroxide) for acetic acid to maximize the polarity differences between Cer(1,3)P and Cer1P.

2.3 RESULTS

Identification of an Optimal TLC Solvent: CHCl₃:MeOH:2N NH₄OH, 60:25:2, v/v/v

Our primary objective in optimizing the TLC solvent system was to develop an assay to achieve separation of this family of sphingolipid metabolites, in particular separation of Cer(1,3)P from its neighboring metabolites, Cer and Cer1P. To do so, a large number of solvent combinations was tested to achieve that separation.

Previously published TLC conditions were initially tried, but they were developed to separate C6-NBD- compounds³³ and the longer chain compounds we used (C12/C11) migrated too high on the silica gel plate. In my BS research option thesis, we had found that the two best solvents for separation of C24-Cer1P, C24-Cer(1,3)P, and C24-SM were CHCl₃:MeOH:H₂O:CH₃COOH (60:20:2:1, v/v/v/v) and CHCl₃:MeOH:H₂O (60:20:2, v/v/v).⁴⁵ Thus, the ratios of these solvents were varied to improve separation of this project's C12/C11 compounds, but none gave sufficient separation of Cer(1,3)P and Cer1P. Next the components were varied with two or more of the following: chloroform, methanol, acetic acid, water, and 2N ammonium hydroxide, and the substitution of ammonium hydroxide for acetic acid caused a large shift in the R_f of the Cer1P but not the Cer(1,3)P. This observation was expected, given that Cer1P has a second dissociable hydroxyl with a pK_a that would enable it to be dianionic under these conditions. After screening these solvents, the optimal TLC solvent was found to be CHCl₃:MeOH:2N NH₄OH, 60:25:2, v/v/v as shown in Figure 2. The main lipid of interest, C12-NBD-Cer(1,3)P, was clearly separated in the middle of the plate from C12-NBD-Cer and C12-NBD-fatty acid (which migrate to the top of the plate but are still separated) and C12-NBD-SM and C11-TopFluor-Cer1P (which migrate to the bottom of the plate but are still separated).

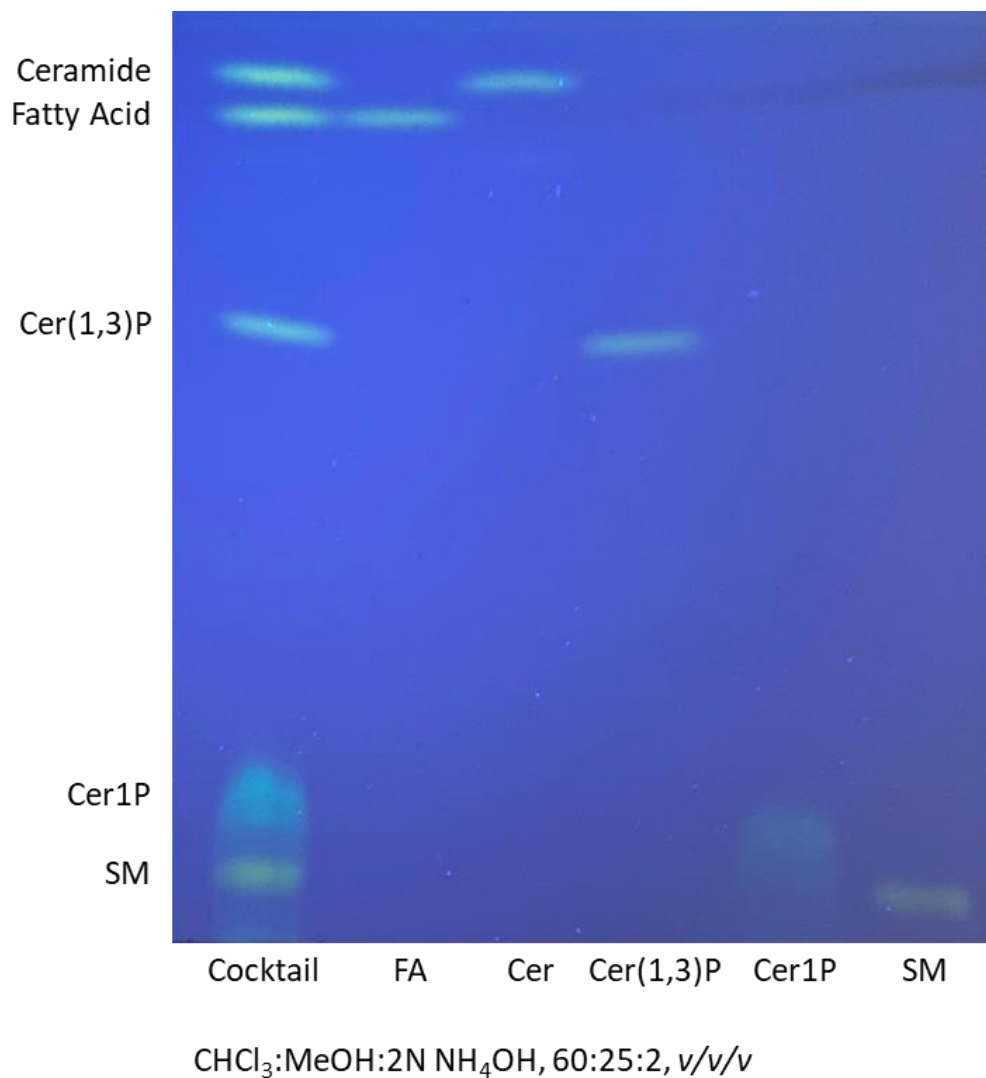


Figure 2. TLC of C12-NBD-Sphingolipid Standards under UV Mineral Light. “Cocktail” is a mixture of each of the five individual NBD-sphingolipid standards (~168 μM). “FA” is C12-NBD-Fatty Acid (12.6 μM), “Cer” is C12-NBD-Ceramide (12.2 μM), “Cer(1,3)P” is C12-NBD-Ceramide(1,3)P (9.1 μM), “Cer1P” a C11-TopFluor-Ceramide 1-P (6.5 μM), and “SM” is C12-NBD-Sphingomyelin (12.6 μM). All are suspended in ethanol.

2.4 DISCUSSION

The elution solvent $\text{CHCl}_3:\text{MeOH}:2\text{N NH}_4\text{OH}$ (60:25:2, v/v/v) was considered optimal because it could be used to clearly distinguish the compounds that are known to be produced by known types of SMases--Cer, Cer(1,3)P and Cer1P--as well as the free fatty acid if a ceramidase activity was also present. Therefore, it could be used to analyze a wide range of biological materials--the spider venoms, bacteria, etc. It does, of course, assume that the enzymes are not so specific for the fatty acyl chain that the fluorescent tag cannot be accommodated, but that has been found for all SMases known to date.

Note that whereas SM, Cer, Cer1P, and FA were tagged with the fluorophore NBD, Cer1P was tagged with TopFluor. We initially planned to use C12-NBD-Cer1P, but found in comparisons of the migration of C24-Cer1P, C12-NBD-Cer1P and C11-TopFluor Cer1P that the migration of these sphingolipids was dependent on their class more than the subtle differences in their side chains (e.g., C12 vs. C11). Therefore, TopFluor was substituted for NBD-Cer1P because it has a slightly different color (blue-tinted versus the greenish-blue fluorescence of NBD) which made its distinction from SM clearer.

We first used solvent systems that contained acetic acid, rather than ammonium hydroxide, based on previous literature.³³ However, Cer(1,3)P and Cer1P migrated very closely together in the acetic acid solvent system and ammonium hydroxide yielded much better separation for our purposes. This difference is attributable to the considerably different polarities of Cer(1,3)P and Cer1P in base because Cer(1,3)P has only one dissociable proton whereas Cer1P has two, for net charges of -1 and -2, respectively.

TLC was chosen over more sophisticated methods to detect sphingolipids, such as high-performance liquid chromatography (HPLC) with fluorescence detection or mass spectrometry, because of TLC's wide availability, ease of use, quicky turnaround, and low cost. A TLC assay was the specific goal because of its power for separating molecules but most especially, the fact that it is a simple methodology available to essentially anybody to perform and can be done rapidly in a laboratory or in a field setting.

With the availability of this analytical system and a cocktail of the pertinent standards, we applied it to known and presumed sphingolipid cleavage activity in spider venoms and bacteria.

CHAPTER 3: VENOM ASSAYS

3.1 INTRODUCTION

With the availability of a method that allows for facile separation of Cer(1,3)P from Cer, FA, SM, Cer1P, we applied it to assay *L. reclusa* venom, for which the production of Cer(1,3)P by the action of SMase D has previously been demonstrated using MS.²⁹ Next, it was applied to *K. hibernalis* venom, for which there had been suggested data that there might be an SMase D,³⁴⁻³⁶ but the presence of such an activity had never been established.

3.2 MATERIALS AND METHODS

Sources of Reagents

The venoms from *L. reclusa* and *K. hibernalis* were obtained from Chuck Kristensen at Spider Pharm (Yarnell, AZ).

Incubations of Venoms with Fluorescent Substrates

The substrate and venoms were prepared as follows: C12-NBD-SM was prepared in 50 mM HEPES buffer at pH 7.5 to yield a 2.4 mM stock. To do so, C12-NBD-SM was added to a 13 x 100 borosilicate glass test tube as an ethanol solution, the solvent was evaporated under nitrogen, then the buffer was added and gently swirled over the lipid film to hydrate it. The test tube was vortexed and sonicated to disperse the C12-NBD-SM as a milky yellow suspension, from which aliquots could be removed for assays. 5 μ L of freeze-dried *L. reclusa* or *K. hibernalis* venom was diluted 1:20 and 1:10, respectively, with 50 mM HEPES buffer, pH 7.5.

For the assay: 10 μ L of substrate and 10 μ L of diluted enzyme were combined in micro Eppendorf tubes and incubated at room temperature for 1 hour. This incubation solution had a C12-NBD-SM concentration of 1.2 mM. 100 μ L of ethanol was added to stop the reaction, and 10 μ L were spotted onto a silica-gel plate. The plate was then developed with the solvent CHCl_3 :MeOH:2N NH_4OH (60:25:2, v/v/v), and products were observed under UV mineral light (long wavelength).

3.3 RESULTS

The Sphingomyelinase D Activity of L. reclusa Venom Produces Only Cer(1,3)P

Using the optimized TLC solvent system and cocktail of standards, *L. reclusa* venom incubated with C12-NBD-SM resulted in nearly complete disappearance of the starting substrate and appearance of only NBD-Cer(1,3)P (Figure 3). Besides confirming that this is the product from the SMase D from *L. reclusa* venom, it is interesting that venom does not appear to contain any additional enzymes that degrade SM or Cer(1,3)P, for example, to produce Cer1P, Cer, or FA.

K. hibernalis Venom Also Contains a Sphingomyelinase D Activity that Results in Cer(1,3)P

Using the optimized TLC solvent system and cocktail of standards, *K. hibernalis* venom incubated with C12-NBD-SM also resulted in some disappearance of the starting substrate and clearly appearance of only NBD-Cer(1,3)P (Figure 3). Thus, this is the first proof that there is sphingomyelinase D activity in *K. hibernalis* venom. It should again be noted that there is no evidence for production of any other metabolites (e.g., Cer1P, Cer, or free FA).

Although these experiments were not intended to provide a quantitative comparison of the levels of activity in these venoms, it is evident that there is much higher activity in *L. reclusa* venom than *K. hibernalis* venom. The *L. reclusa* venom was twice as dilute (1:20) as the *K. hibernalis* venom (1:10), yet, the *L. reclusa* venom appears to have completely hydrolyzed the SM whereas *K. hibernalis* venom converted only a fraction (probably no more than 10%) of the C12-NBD-SM to C12-NBD-Cer(1,3)P. Therefore, this assay indicates that *L. reclusa* venom is at least an order of magnitude—and very likely even more—potent in SMase D activity than *K. hibernalis* venom.

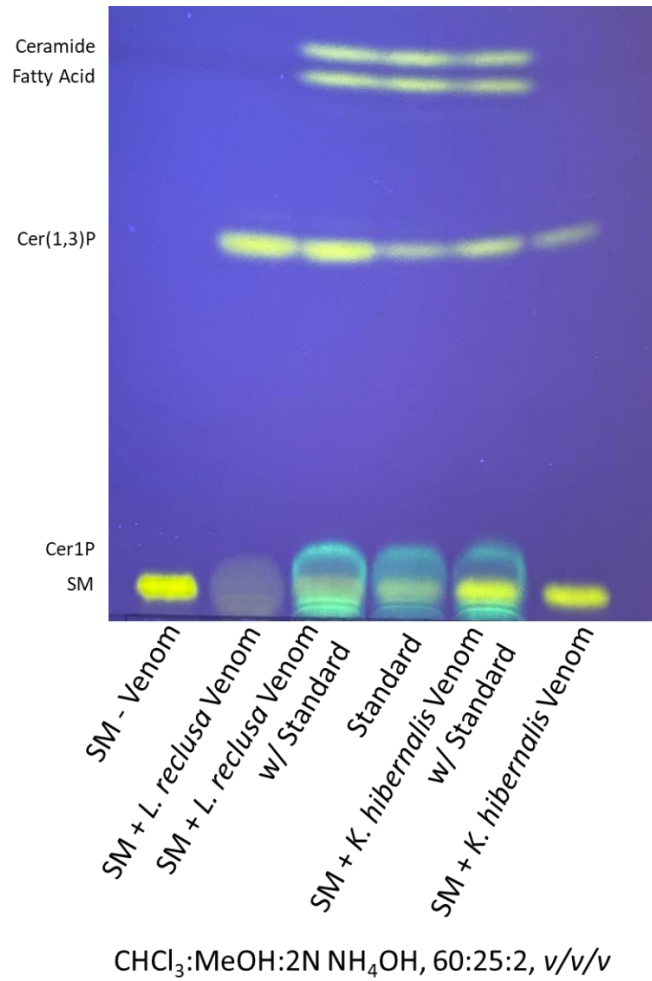


Figure 3. TLC of Incubations of *L. reclusa* and *K. hibernalis* Venom with NBD-SM under UV Mineral Light. NBD-SM (1.2 mM) was combined with a diluted enzyme source, in the form of *L. reclusa* or *K. hibernalis* venom. These samples were incubated for 1 hour, at which time the reaction was stopped with ethanol. The ethanol mixture was spotted onto a silica gel plate and run in the stated solvent.

3.4 DISCUSSION

For about a decade, the sphingomyelinase D in the venom of *L. reclusa* has been known to produce cyclic Cer(1,3)P²⁹ but there have been relatively few studies of this compound, possibly because there were few synthetic standards available and because the method of analysis (mass spectrometry) was not widely accessible. This is unfortunate because Cer(1,3)P is a very interesting compound since it resembles other “signaling” sphingolipid metabolites (e.g., Cer and Cer1P), and it appears that human cells cannot readily degrade it. The simple assay developed for this thesis readily confirmed that the SMase D in *L. reclusa* venom cleaves SM to yield Cer(1,3)P.

It is also sensible to wonder if Cer(1,3)P can be produced by other spider venoms, such as *K. hibernalis*, which has a relatively uncharacterized mechanism of toxicity. Our assay also showed that that *K. hibernalis* cleaves SM to yield Cer(1,3)P, experimentally suggesting that *K. hibernalis* could possess a similar or closely related sphingomyelinase D to that of *L. reclusa*. This has been a long-going project of the Merrill laboratory, starting with the finding by undergraduate students that incubation of venoms from several spider species (including *K. hibernalis* and *L. reclusa*) resulted in disappearance of the substrate SM. However, production of Cer1P could not be confirmed, which was explained by the report that the breakdown product of *L. reclusa* venom is actually Cer(1,3)P.²⁹ Therefore, it is now satisfying to be able to confirm that Cer(1,3)P is produced by *K. hibernalis* venom.

These findings are also consistent with the report that an enzyme-linked immunosorbent assay (ELISA) to detect the presence of *Loxosceles* spiders found antigenic cross reactivity with *K.*

hibernalis venom.³⁴ This might also help explain why a few cases of dermonecrosis have been reported after *K. hibernalis* bites.³⁶ A defining characteristic of *L. reclusa* spider bites is dermonecrosis.

Despite finding this activity in the venom from *K. hibernalis*, the activity was much lower than for *L. reclusa* venom, which also corresponds to the general perception that the effects of *K. hibernalis* spider bites are relatively mild. This might be due as well to the many factors that determine the potency of venom, such as the ability of the spider fangs to penetrate skin, the venom volume that is delivered by the spider, and concentration of the toxic components of the venom. Perhaps in cases where dermonecrosis results in individuals bitten by *K. hibernalis*, the spiders are expressing a more potent form of the enzyme or have a higher amount of the enzyme in their venom. The affected individual might also have been more sensitive.

Now that there is a facile way to determine if spider venoms cleave SM to Cer(1,3)P, it will be interesting to explore how widespread these activities are among different spiders and other organisms.

CHAPTER 4: ISOLATED BACTERIA ASSAY

4.1 INTRODUCTION

Bacteria have a wide spectrum of phospholipases that are important, including some that are engaged in sphingolipid metabolism. The assay we have developed is helpful in addressing questions of whether bacteria have sphingomyelin cleavage activity that could result in the production of Cer(1,3)P. To identify organisms that could fall into the aforementioned category, we assayed soil bacteria that we grew on media supplemented with SM and Cer(1,3)P as sole carbon and energy sources. Our goal was to get an enrichment of bacteria with activities to metabolize these substrates.

4.2 MATERIALS AND METHODS

Sources of Reagents

The C12-Cer (catalog # 860512), C24-Cer (catalog # 860524), C12-Cer1P (catalog # 860531) and C24-Cer1P (catalog # 860527), C6-Cer(1,3)P (catalog # 860704), and C12-Cer1,3P (catalog # 860702) were obtained from Avanti Polar Lipids (Alabaster, AL).

Bovine buttermilk SM (#1329) was obtained from Matreya, LLC (State College, PA).

Growth medium salts (potassium phosphate [K₂HPO₄], # JT3246-1 and sodium phosphate [Na₂HPO₄], #JT3828-01; ammonium chloride, #15186674 and sodium chloride, # S271-1) were obtained from VWR (West Chester, PA) and Fisher Scientific (Waltham, MA), respectively. The supplement magnesium sulfate (MX0070-1) in the growth media was obtained from Millipore Sigma (Burlington, MA). Thiamine hydrochloride (#T4625-5G) was obtained from Sigma-Aldrich (St. Louis, MO). Bacto Agar (#214010) used in making solid growth medium was obtained from VWR (West Chester, PA).

The 1X Dulbecco's phosphate-buffered saline (DPBS) without calcium and magnesium (#21-031-CV) was obtained from Corning (Manassas, VA).

Syntheses

C24-Cer(1,3)P was synthesized from C24-Cer1P by essentially the method published by Boudker and Futerman,³³ except that pyridine was used instead of DMF as the solvent because the longer chain Cer1P was not soluble in DMF. Its identity was established by mass spectrometry and co-migration on TLC with the Cer(1,3)P standards obtained from Avanti Polar Lipids (Alabaster, AL).

Growth Medium (Liquid Medium)

First, 5X M9 salts were prepared, consisting of 22 mM KH_2PO_4 (anhydrous), 42 mM Na_2HPO_4 (anhydrous), 0.86 mM NaCl , and 1.87 mM NH_4Cl .⁴⁶ These salts were dissolved in 1 L of dH_2O and autoclave sterilized.

To prepare M9 minimal medium, the following solutions were combined, with their final concentrations listed in parenthesis: 5X M9 salts (1X), 1M MgSO_4 (2.0 mM), 1M CaCl_2 (0.1 mM), thiamine (vitamin B_1) (0.01%), and trace metals (1X).⁴⁶ Thiamine (1%) was prepared by dissolving 1 mg in 1 mL of DI water and then filter sterilizing the solution through a 0.22- μm filter. The trace metal solution (1X) was prepared according to Table 1. For negative control samples, no carbon source was added. For all other samples, the carbon source of interest was added before bringing the above M9 minimal medium solution up to 1 L. When used, glucose or glycerol was added to a final concentration of 0.4%. The addition of dH_2O resulted in 1 L solution.

Alternatively, SM (final concentration of 0.01%) was used as a carbon source instead of glucose. Please see “Preparation of Sphingolipid Liposomes for Addition to Growth Medium” for the preparation of SM for addition to growth medium. Addition of SM to growth medium was done in a three-step process. The first solution of growth medium had a 10 mg/mL concentration of SM which was sonicated (Branson 1510 Ultrasonic Cleaner) in warm water for one hour. The next growth medium dilution had an SM concentration of 1 mg/mL, which was sonicated for one hour, and the final dilution had an SM concentration of 0.1 mg/mL and was also sonicated for one hour.

Cer(1,3)P (final concentration of 0.01%) was another carbon source in liquid media, added to growth medium similarly to SM.

Table 1. 100X Trace Elements Solution.⁴⁷

Ingredient	Amount of Stock	Final Concentration
EDTA	5 g/L	13.4 mM
FeCl ₃ -6H ₂ O	0.83 g/L	3.1 mM
ZnCl ₂	84 mg/L	0.62 mM
CuCl ₂ -2H ₂ O	13 mg/L	76 μM
CoCl ₂ -2H ₂ O	10 mg/L	42 μM
H ₃ BO ₃	10 mg/L	162 μM
MnCl ₂ -4H ₂ O	1.6 mg/L	8.1 μM

This 100X trace elements stock solution was prepared for use at 1X. Five grams of EDTA was dissolved into 800 mL of water. pH was adjusted to 7.5 with NaOH. Other ingredients were combined at these specified amounts, and DI water was added to yield a final volume of 1 L. The solution was sterilized over a 0.22-μm filter.

Agar Plates (Solid Medium)

For M9 minimal medium agar plates (1 L), 5X M9 salts (1X) was combined with 15 g of Bacto-agar (1.5% agar). dH₂O was added to bring the solution up to 1 L. This solution was autoclave-sterilized. After the sterilized solution was cooled to 50°C or less, sterile solutions of 1M MgSO₄ (2.0 mM), 1M CaCl₂ (0.1 mM), thiamine (vitamin B₁) (0.01%), and trace metals (1X) were added to the M9 salts (1X) and Bacto-agar mix.⁴⁶ A carbon source was either added at this stage or spread onto plates that did not contain a carbon source prior to using the plate; omission of a carbon source from the plate allowed for the carbon source to be added just prior to using the plate. The cooled medium (50°C or less) was then poured into 15mm x 100mm petri dishes. Average plate volume was estimated and carbon source spread to a plate at the following concentrations: glucose or glycerol (final concentration of 0.4%), SM (0.01%), or Cer(1,3)P (0.01%).

Preparation of Sphingolipid Dispersions for Addition to Growth Medium

The bovine buttermilk SM was prepared for use as the sole carbon source in growth medium to isolate bacteria. The desired amount of SM was weighed into sterile Pyrex 16 x 100 mm borosilicate screw-capped glass test tubes. SM was then dissolved in several milliliters of CHCl₃:EtOH, 2:1, v/v. The test tube containing the SM and solvent was then placed into a clamp holder which was attached to a clamp stand. Resting in a warm water bath, the test tube had a dry nitrogen stream blown into it with enough intensity to distribute the lipid throughout the bottom of the test tube. After removing the solvent with the stream of nitrogen gas, the test tubes were placed into a desiccator that was vacuum pumped for at least one hour. The desiccator was sealed, and the tubes were left under negative pressure overnight.

The next day, the test tubes were removed from the desiccator. 1X Dulbecco's phosphate-buffered saline (DPBS) was added to the test tubes for 5 mg/mL. The test tubes were placed in a gently shaking water bath at a temperature above the phase transition of SM (55 to 65°C). The mixture was allowed to hydrate for about one hour with occasional vortexing. The test tubes were then placed in a bath sonicator (Branson 1510 Ultrasonic Cleaner), filled with warm water for 30 to 60 min to disperse the SM further. Consistent with this, the appearance of the solution in the test tube changed from milky to more translucent after sonication. At this point, the solution was ready to be added to growth medium and treated as indicated above.

Isolation Process for Soil Bacteria

This isolation process is outlined in Figure 4. Soil was collected from outside the Ford Environmental Science & Technology Building (33.779036, -84.395639; 311 Ferst Dr NW,

Atlanta, GA 30332) on the campus of the Georgia Institute of Technology. The soil was homogenized by being broken up and mixed.

Since SM was more available/abundant, SM was used initially as a restrictive carbon source in the hopes of later selecting more specifically for Cer(1,3)P degraders. Soil (1% w/v) was used to inoculate M9 media containing 0.01% SM as the sole carbon source in 50-mL Erlenmeyer flasks. Additionally, 1% (w/v) soil was placed into aluminum foil packets and autoclaved; this soil served as the abiotic control. Half of the samples were left to incubate in an environmental room set to 35°C, and the other half incubated at room temperature. All samples incubated on a shaker at 150 rpm for aeration.

Growth of the samples during the initial isolation of soil bacteria on a restrictive carbon source was assessed with optical density (OD). Though, it should be noted that the vesicles of sphingolipids such as SM may confound the OD readings (i.e., higher values may not indicate an increase in growth in this case, as they typically do in other cases). One-mL aliquots from each sample were taken and placed into 1.5-mL cuvettes (#14955127; Fisher Scientific; Pittsburgh, PA). A spectrophotometer (#DR2800-01B1; Hach Company; Loveland, CO) read each sample at the single wavelength of $\lambda = 600$ nm. The spectrophotometer was blanked with the same media as that used in the samples. OD readings were taken every day.

To further purify the enrichment culture, transfers to fresh media were made. When a transfer was made, OD readings were taken before and after the transfer. Cells from the current culture were transferred in a 1:100 dilution to fresh flasks of the same type of growth medium. Every few transfers, the remaining soil cultures that were not transferred were pelleted at 10000 rpm for 5 minutes, resuspended in some medium, and saved as glycerol stocks (20% glycerol) in a -80°C freezer, rather than discarded.

At the end of the two-month isolation period, the remaining soil cultures were pelleted in 15-mL conical tubes at 3400 rpm for 15 minutes. The pellets were resuspended in ~1 mL of residual conical tube medium and were then transferred to microcentrifuge tubes. The resuspended pellet in the microcentrifuge tube was centrifuged at 10000 rpm for 2 minutes. These pellets were saved as glycerol stocks (20% glycerol) in a -80°C freezer.

Near the end of the two-month isolation period, dilutions (e.g., 10^{-4} , 10^{-5} , 10^{-6}) of the soil cultures were plated onto M9+SM agar (0.01% SM) and incubated at their respective temperatures of isolation (i.e., 35°C or RT). Plating on solid medium allowed for easier identification of distinct bacterial phenotypes (e.g., colony morphology, pigment, etc.). To ensure growth on the substrate SM, single colonies were selected from these dilution plates and were plated onto other M9+SM agar (0.01% SM) plates. Single colonies from these second plates were saved as separate glycerol stocks (20% glycerol) in a -80°C freezer.

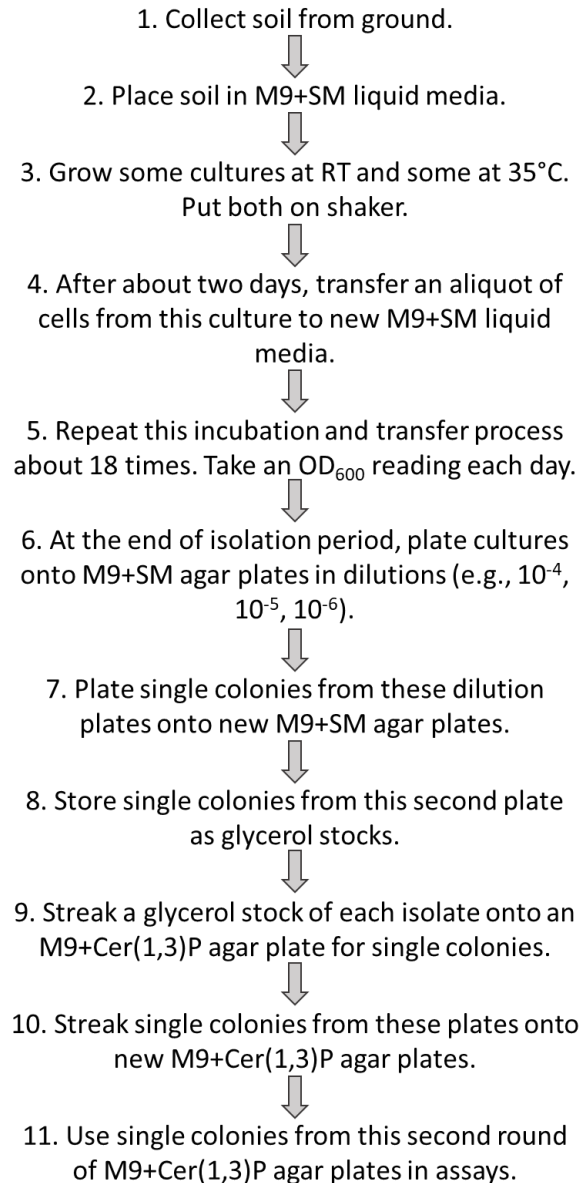


Figure 4. Soil Bacteria Isolation Process. Bacteria from the soil were initially isolated on the more abundant carbon source of SM and then screened on the main carbon source of interest, Cer(1,3)P. These steps were taken for use of the isolates in downstream application in assays.

Preparation for Analysis of Protein Concentration and Lipids Present over Time

Glycerol stocks of the isolates were streaked for single colonies onto an M9+Cer(1,3)P (0.01%) plate (see steps 8 – 11 of Figure 4). A single colony from this plate was streaked out onto a new

M9+Cer(1,3)P (0.01%) plate. To achieve enough biomass, cells were initially grown up in a culture of glucose before being grown on a restrictive carbon source. An M9+glucose (4%) culture was inoculated with a single colony from this second plate and grew while shaking at 150 rpm. Cultures were inoculated in triplicate for each of the two isolates. After four days of growth and achieving a high enough growth density, a 1:10 dilution was removed from these cultures to be added to new media. Before inoculating the new media, these cells were spun down at 3400 rpm for 15 minutes, washed in 1X PBS, and spun down at 3400 rpm for 15 minutes. To attempt to induce cells to express enzymes that have sphingomyelinase activity, these cells were then suspended in the new media of M9+Cer(1,3)P (0.05%) to grow while shaking at 150 rpm. Cells grown in the M9+Cer(1,3)P (0.05%) media were assayed. Immediately, 1.1 mL of this new culture was put into a cuvette, and an OD (at $\lambda = 600$ nm) reading was taken. This was T_0 . Subsequent time points were taken every day for about one week. After an OD reading was taken, 1 mL of culture from the 1.1 mL in the cuvette was placed into a microcentrifuge tube and spun down at 15000 rpm for 1 minute. The supernatant was removed, and the pellet was stored in a -80°C freezer. This was done for each time point.

Additional 1-mL aliquots of the time 0 and last time point were spun down at 3400 rpm for 15 minutes. The supernatant was then removed and saved separately from the pellet. Lipids of the supernatants and pellets of the first and last time points of isolate growth on the sole carbon source of Cer(1,3)P were extracted and run on silica-gel plates, visualized with iodine staining.

Assaying Protein Concentration over Time

Protein concentration was assayed using the test tube procedure of the Pierce BCA Protein Assay Kit (#23227; Thermo Fischer Scientific; Waltham, MA). The day that the assay was done, BSA standards were prepared the same way as samples to create a standard curve.

Pellets that had been stored in the -80°C freezer were lysed by addition of 1M NaOH to each pellet to break open the cells and release the proteins. After mixing well, samples were placed in a heating block set to 60°C for 15 minutes. The samples were then spun down at 15000 rpm for 1 minute. Since the lysate contained the proteins, it was removed and placed into a fresh microcentrifuge tube. The volume was brought up with dH_2O , creating a 0.5 M NaOH solution. The samples were then ready for use in the assay.

BSA standards were prepared as described in Table 2. They were then prepared in the exact same conditions as the samples. NaOH was combined with each of the six standards to make 0.5M NaOH solutions, resulting in a final volume equal to that of the samples. After mixing well, samples were placed in a heating block set to 60°C for 15 minutes. Working reagent was prepared according to the protocol (Enhanced Protocol: 60°C for 30 minutes).

A standard curve was prepared from the BSA standards, and protein concentration could then be determined in the samples at a given time point.

Table 2. BSA Dilutions and Final Concentrations.

Vial	Volume of Diluent (μL)	Volume & Source of BSA (μL)	BSA Concentration ($\mu\text{g}/\text{mL}$)	BSA Concentration with NaOH Addition ($\mu\text{g}/\text{mL}$)
A	700	200 of Stock*	500	250
B	400	400 of Vial A dilution	250	125
C	450	300 of Vial B dilution	100	50
D	400	400 of Vial C dilution	50	25
E	400	100 of Vial D dilution	10	5
F	400	0	0 \rightarrow Blank	0 \rightarrow Blank

Note that if BSA standard solutions are diluted from 1x to 0.5x (50 μ L \rightarrow 100 μ L) with 1 M NaOH, 2x as much stock (200 μ L instead of 100 μ L) must be used initially to achieve the same final BSA concentrations. The Pierce BCA Protein Assay Kit protocol indicates to use 100 μ L of BSA stock, but an adjustment was made here to 200 μ L of BSA stock since the BSA standards are diluted with 1 M NaOH in this case. Otherwise, all final BSA concentrations will be halved.

Preparation for Incubations of Isolates with Fluorescent Substrates

Fifteen mL of M9+glucose medium was inoculated with a single colony of isolate 6 or 7 from an M9+Cer(1,3)P agar plate. Cultures were grown for two days by shaking at 150 rpm at room temperature. Ten mL of each sample was centrifuged at 3400 rpm for 15 minutes. Four mL of supernatant was placed into an Amicon Ultra-4 Centrifugal Filter tube (Millipore Sigma; Burlington, MA) which was centrifuged at 4000 rpm for 20 min. The concentrated protein was then placed into an Eppendorf tube. The remaining supernatant was removed and pellets were resuspended in 1 mL of 1X PBS.

Incubations of Isolates with Fluorescent Substrates

Ten μ L of cell-free M9+glucose media, the concentrated supernatant, and the pellet were incubated separately with 10 μ L NBD-C12-SM (1.2 mM) and 10 μ L NBD-C12-Cer(1,3)P (0.35 mM), yielding six samples per isolate. NBD-C12-SM and NBD-C12-Cer(1,3)P were suspended in 50 mM HEPES buffer, pH 7.5. After one hour of incubation, half of the sample volume (10 μ L) was removed and 50 μ L of ethanol was added to stop the reaction. These samples were spotted on TLC plates along with standards and run in the solvent CHCl₃:MeOH:2N NH₄OH, 60:25:2, v/v/v and observed under UV mineral light (long wavelength). After 24 hours, 50 μ L of

ethanol was added to the other half of the samples that continued to react. These samples were run via TLC in the same solvent and observed under UV mineral light (long wavelength).

Protein Assay of Fluorescent Substrate Incubations

Protein concentrations of the samples were assayed via BCA assay, using a standard curve of BSA. A new standard curve of BSA was prepared similarly to the one previously described, but without the addition of NaOH or application of a heating block. Samples from cell-free M9+glucose medium, dilutions of concentrated supernatants, and dilutions of cell pellets were then assayed for protein concentration in the same way as the BSA (with no addition of NaOH and no time spend in a heating block). Dilutions were made to measure protein concentration within the range of the assay (0 – 250 $\mu\text{g/mL}$).

4.3 RESULTS

Growth of Isolates on Cer(1,3)P Solid Medium Plates Shows Possible Cer(1,3)P Cleavage

Over the course of two months (09-25-2020 to 11-23-2020), a microbial enrichment was obtained from soil under aerobic conditions with SM as the sole carbon and energy source. Every other day, a transfer of the current soil cultures to fresh media was made to enrich for only sphingolipid users. A total of 24 transfers was made to enrich for only sphingolipid degraders, as earlier passages may have had bacteria that took advantage of dying cells for growth. After plating isolate 6 onto M9 agar medium containing different carbon sources (C6-Cer(1,3)P, C6-Cer(1,3)P + glucose, glucose, and no carbon source), we observed growth on plates containing Cer(1,3)P + glucose, glucose, and no carbon source, but not on plates that do not have a carbon source (Figure 5). The bacteria were initially isolated on SM in liquid culture as well. The initial isolation of the bacteria on SM and this isolate's apparent ability to metabolize Cer(1,3)P as a carbon source indicate that at least isolate 6 has an activity to metabolize sphingolipids. However, the isolate may only be able to perform this activity under certain conditions, such when a biofilm can be formed or when this activity can be induced with a sphingolipid.



Figure 5. Isolate 6 Growth on M9 Agar Medium Containing Different Carbon Sources.

Petri dishes containing M9 agar were supplemented with the listed carbon sources and then

grown at room temperature for several days. The Cer(1,3)P used is C6. Note that there is growth of isolate 6 on the plate containing Cer(1,3)P only, and there no growth of the isolate on the plate without a carbon source.

Non-Fluorescent Substrate Assay Does Not Show Cer(1,3)P Cleavage in Isolates

Isolates 6 and 7 were grown in Cer(1,3)P media for about five days. Cells were initially grown in media containing glucose to achieve enough biomass but were then washed in PBS to remove any residual glucose and transferred to Cer(1,3)P growth medium. A standard curve of BSA for identification of protein concentration in the isolates was made in the same conditions under which samples were subjected in the assaying of their protein concentrations (Figure 6). Each time point was assayed for protein concentration, which was determined by the standard curve (Figure 7). Lipids from the initial (time 0) and last time points were extracted from pellets and supernatants of the growth medium (Figure 8). The decrease in protein concentration over time and unnoticeable change in lipids present between the initial and last time points do not provide evidence that isolates 6 and 7 can cleave Cer(1,3)P.

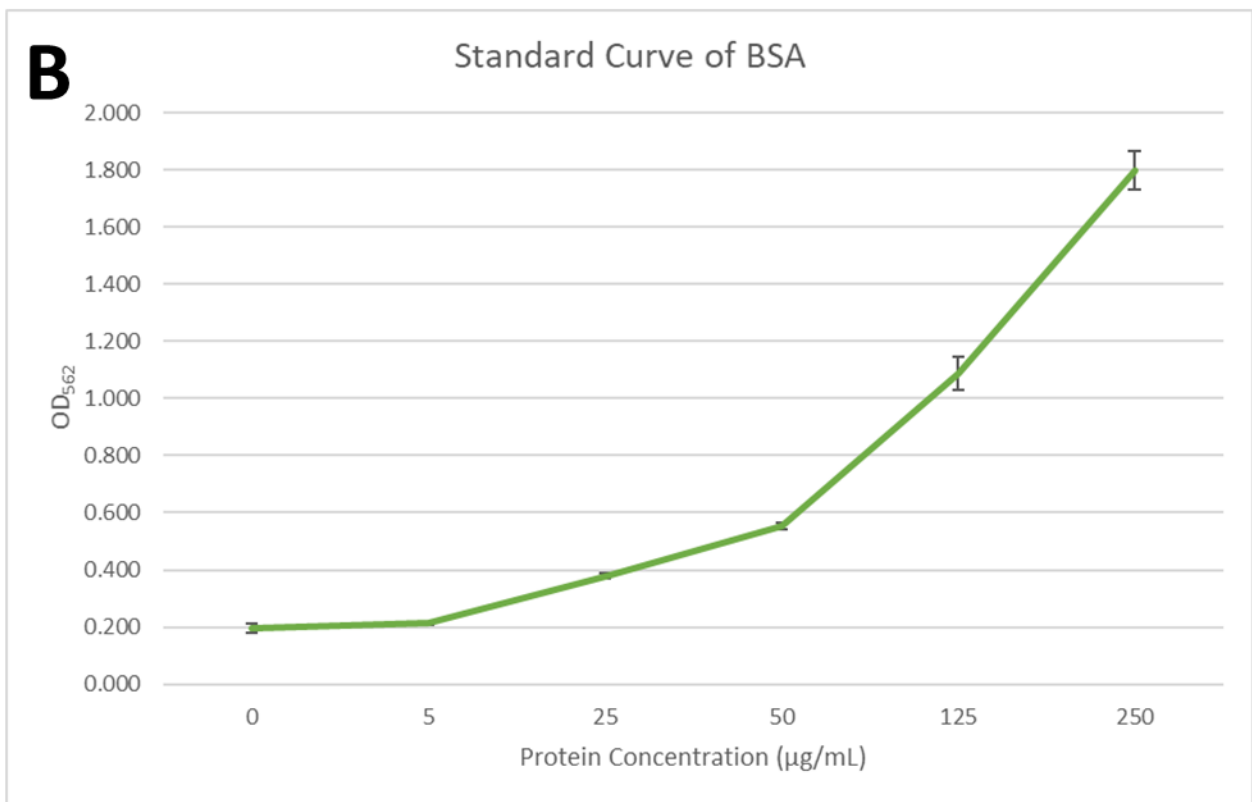
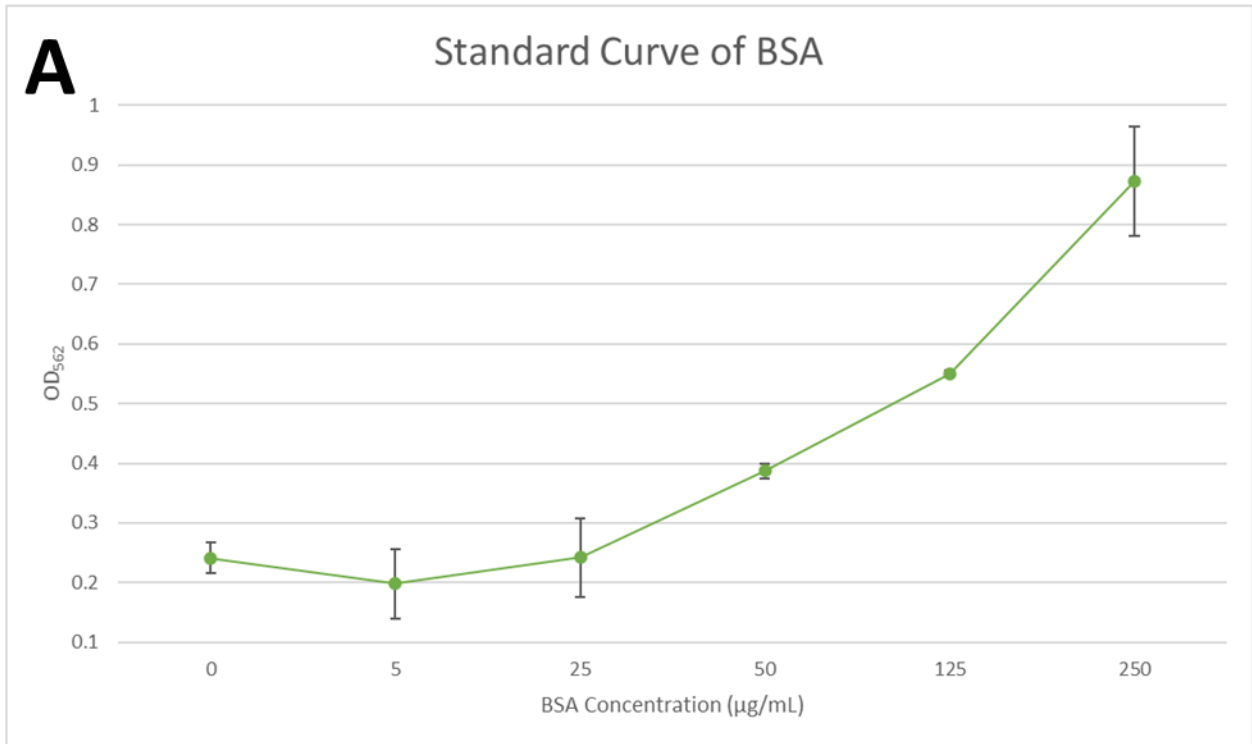
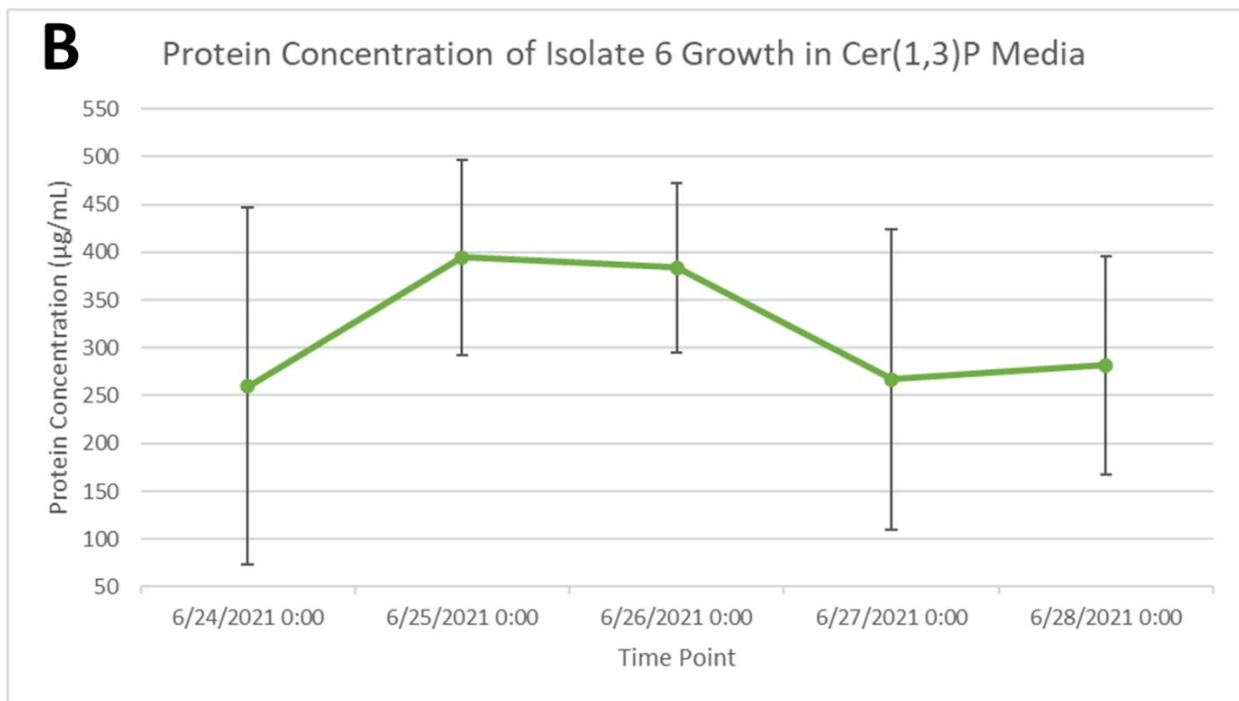
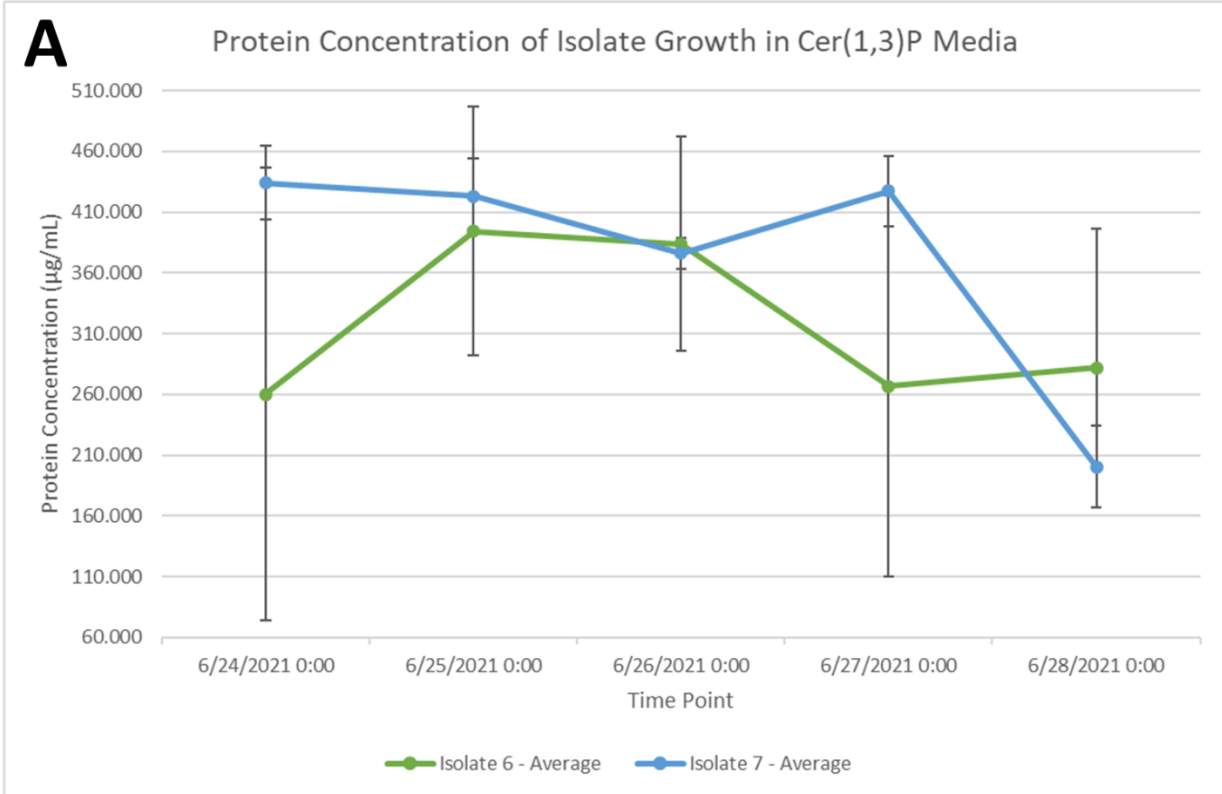


Figure 6. Standard Curve of BSA. (A) represents a standard curve for the non-fluorescent substrate growth and is described by the following. In triplicate, BSA solutions were prepared at

the above concentrations to the method by which the samples of unknown protein concentration were prepared. The averages of triplicates at BSA concentrations are shown, and error bars represent the standard deviation of the three replicates. (B) represents a standard curve for the fluorescent substrate incubations and is described by the following. In triplicate, BSA was prepared at the above concentrations identically to the method by which the samples of unknown protein concentration were prepared (in this case without the addition of NaOH and without the application of heat). The averages of triplicates at BSA concentrations are plotted on the graph, and error bars represent the standard deviation of the three replicates.



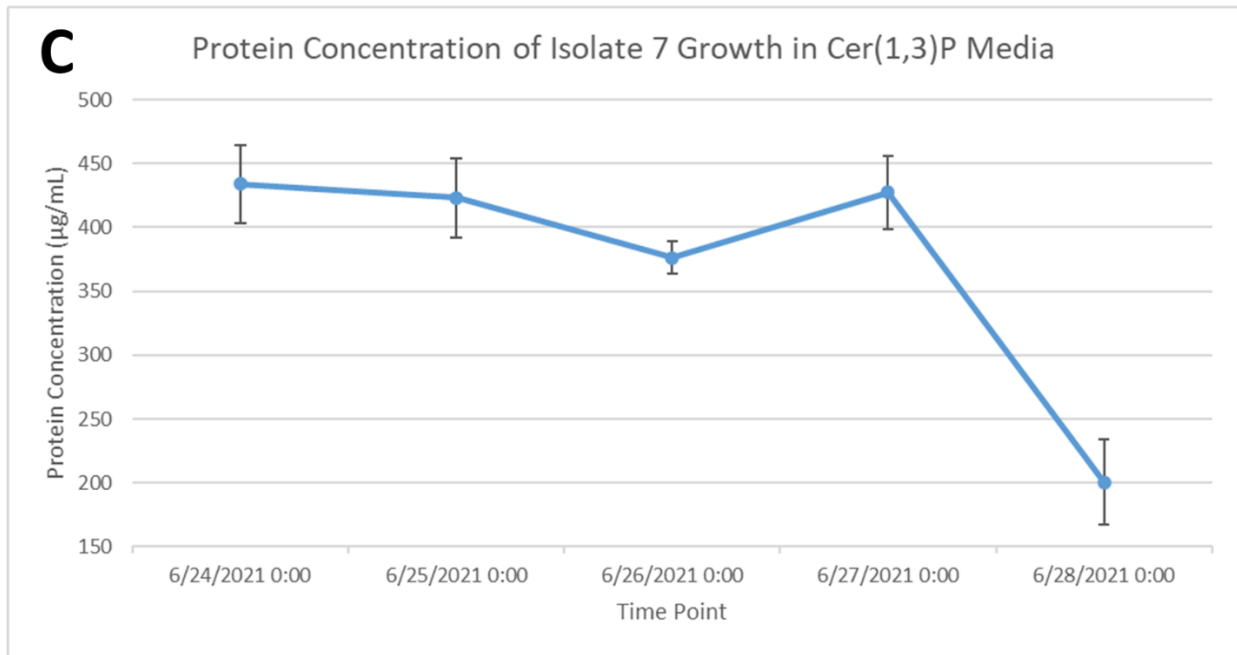


Figure 7. Protein Concentration of Isolate Growth in Media with Cer(1,3)P as the Sole

Carbon Source. From their respective frozen glycerol stocks, isolates were streaked for single colonies onto plates with Cer(1,3)P as the sole carbon source. A single colony was taken from this plate and then streaked for single colonies onto a new plate with Cer(1,3)P as the sole carbon source. Single colonies were taken from this second plate and used to inoculate media with glucose as the sole carbon source in triplicate. After the cultures grew, a 1:10 dilution of cells was washed in PBS and then added to media with Cer(1,3)P as the sole carbon source. The graph represents the protein concentrations for time points of this culture over the course of a few days. The protein concentration has been determined with a BCA assay, which compares optical densities of these samples to those of standards (BSA) at known protein concentrations. The averages of triplicates for each of the two isolates are plotted, and error bars represent the standard deviation of the three replicates. Graph A contains both isolates 6 and 7. Graph B contains isolate 6 only. Graph C contains isolate 7 only. Since protein concentration shows a decreasing trend in both isolates 6 and 7 when they were grown on growth medium

supplemented with Cer(1,3)P as the sole carbon source, there is no evidence from this protein assay that the isolates are metabolizing and breaking down the Cer(1,3)P.

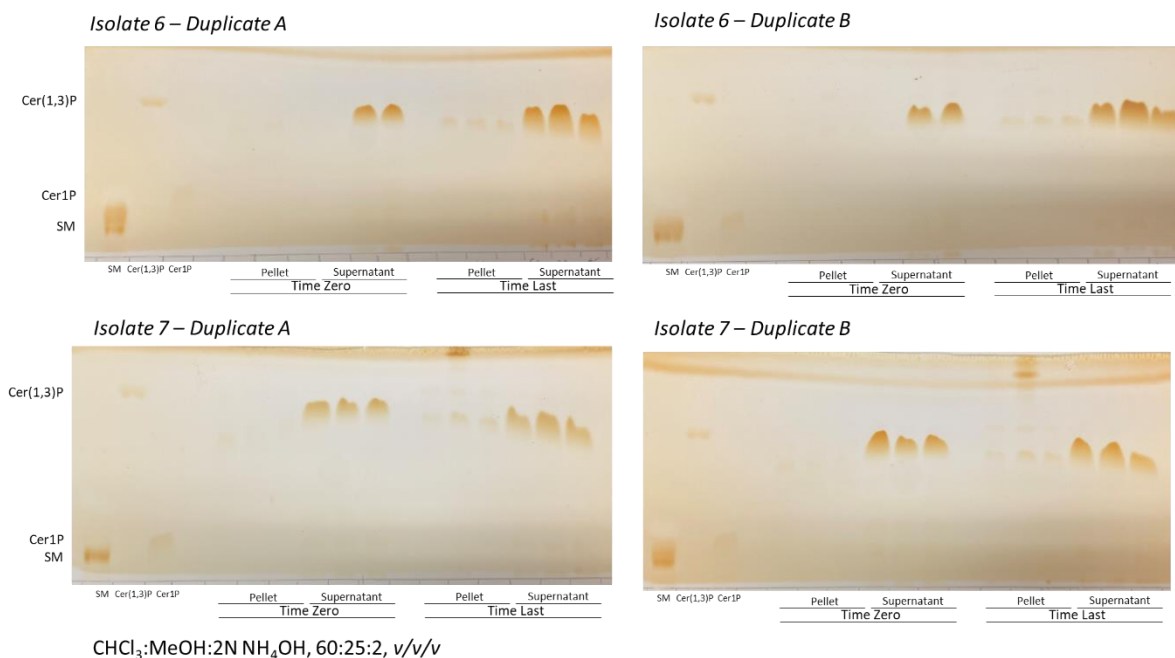


Figure 8. TLC of Isolates 6 and 7 Growth on C8-Ceramide(1,3)P over Time with Iodine Staining. An M9+glucose (4%) culture was inoculated with a single colony from an M9+Cer(1,3)P (0.01%) plate. Cultures were inoculated in triplicate for each of the two isolates. After four days of growth, a 1:10 dilution was removed from these cultures to be added to new media. Before inoculating the new media, these cells were spun down at 3400 rpm for 15 minutes, washed in PBS, and spun down at 3400 rpm for 15 minutes. These cells were then suspended in the new media of M9+Cer(1,3)P (0.05%). A time point (time zero) was taken at initial inoculation. Subsequent time points were taken about every day. The first and last time point aliquots were spun down at 3400 rpm for 15 minutes. The supernatant was removed and saved separately from the pellet. Lipids of the supernatants and pellets of the first and last time points of isolate growth on the sole carbon source of Cer(1,3)P were extracted and are

represented in this figure by TLC, visualized with iodine staining. Shown in the figure are isolates 6 and 7, with TLC plates in duplicate. Each sample is represented in triplicate, except for the supernatant time zero sample for isolate 6 which is represented in duplicate. Supernatants and pellets are shown in triplicate.

Fluorescent Substrate Incubation Does Not Show SM or Cer(1,3)P Cleavage by Bacteria

Isolates 6 and 7 were grown in M9+glucose medium overnight. An aliquot was removed, and its supernatant proteins were concentrated in the event that the enzyme of interest was secreted; a concentrated amount would allow for a faster assay. A standard curve of BSA was made in the same conditions under which samples were subjected (Figure 6). Pelleted cells and the concentrated supernatants were assayed for protein concentration (Figure 9). The supernatants, pellets, cell-free media were then incubated with NBD-SM or NBD-Cer(1,3)P, and the incubation products were analyzed at 1 hour and at 24 hours (Figure 10). Assays indicated no disappearance or new appearance of any fluorescent sphingolipid. Therefore, this assay does not show evidence of SM or Cer(1,3)P cleavage in isolates 6 and 7.

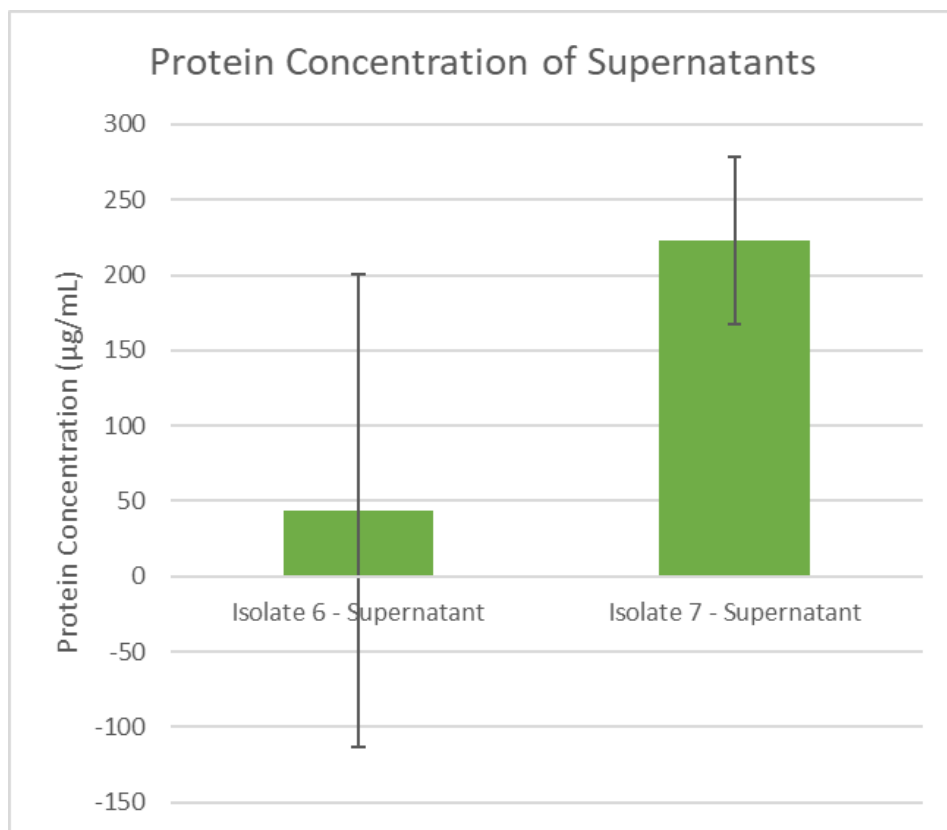
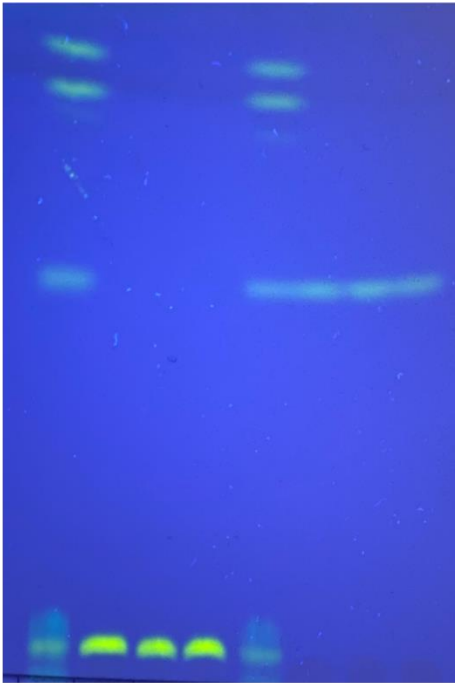


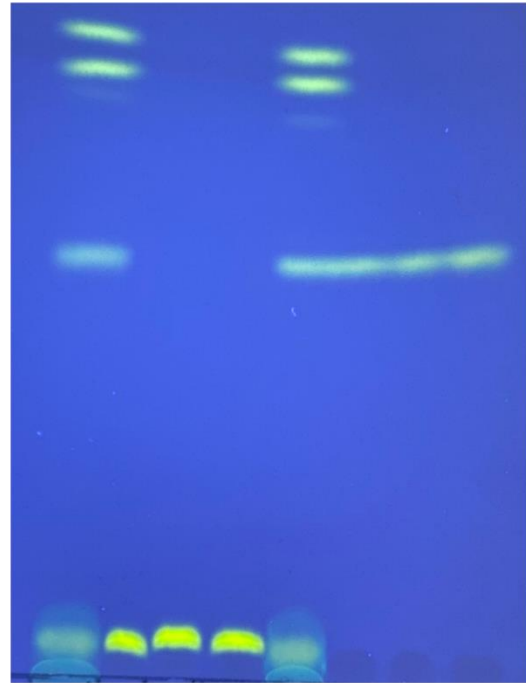
Figure 9. Protein Concentration of Supernatants. Protein concentrations of supernatants of isolates 6 and 7 were determined via BCA assay. This graph represents the protein concentrations of isolates that were then incubated with NBD-SM and NBD-Cer(1,3)P. Protein concentration of pellets and media was also assayed similarly but was too high and therefore the values could not be extrapolated beyond the assay's dynamic range.

Isolate 6 – 1 Hour



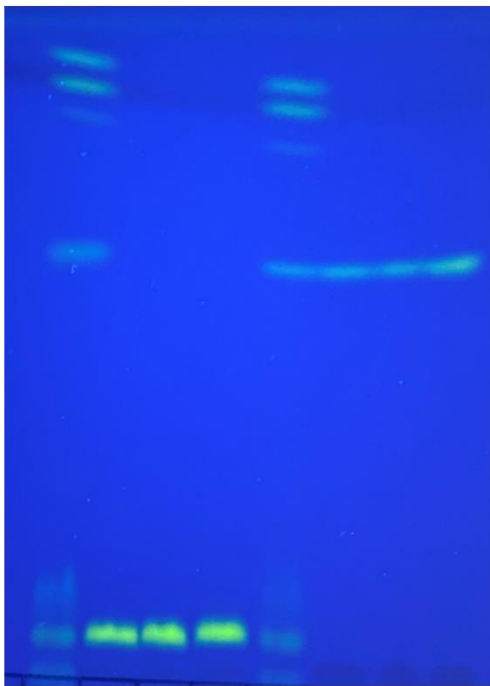
M S P M S P
SM Incubation Cer(1,3)P Incubation

Isolate 6 – 24 Hour



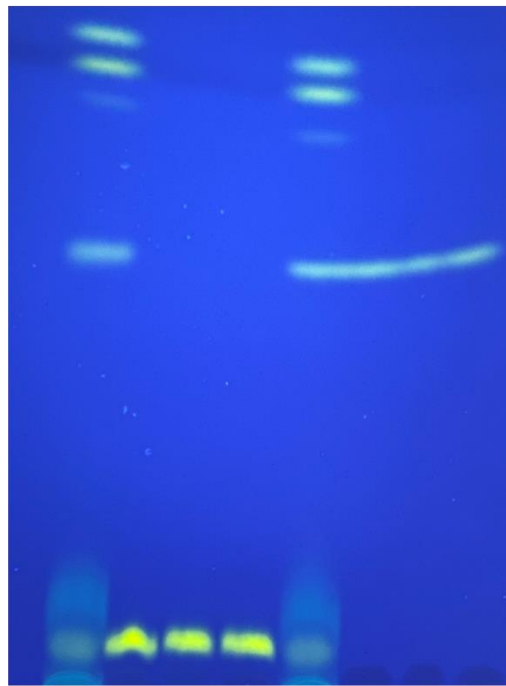
M S P M S P
SM Incubation Cer(1,3)P Incubation

Isolate 7 – 1 Hour



M S P M S P
SM Incubation Cer(1,3)P Incubation

Isolate 7 – 24 Hour



M S P M S P
SM Incubation Cer(1,3)P Incubation

CHCl₃:MeOH:2N NH₄OH, 60:25:2, v/v/v

Figure 10. TLC of Incubations of Isolates 6 and 7 with NBD-SM and NBD-Cer(1,3)P at 1 Hour and 24 Hours under UV Mineral Light. M9+glucose medium was inoculated with a single colony of isolate 6 or 7 from an M9+Cer(1,3)P agar plate. Supernatant was placed into an Amicon Ultra-4 Centrifugal Filter tube which was centrifuged. The remaining supernatant was removed from the spun-down culture, and pellets of these cultures were resuspended in 1X PBS. Cell-free M9+glucose media (M), the concentrated supernatant (S), and the pellet (P) were incubated separately with NBD-C12-SM (1.2 mM) and NBD-C12-Cer(1,3)P (0.35 mM), yielding six samples per isolate. NBD-C12-SM and NBD-C12-Cer(1,3)P were suspended in 50 mM HEPES buffer, pH 7.5. After one hour of incubation, half of the sample volume was removed, and ethanol was added to stop the reaction. These samples were spotted on silica gel plates and run. After 24 hours, ethanol was added to the other half of the samples that continued to react. These samples were run via TLC in the same solvent. The first lane on each plate is the standard cocktail.

4.4 DISCUSSION

Using the assay developed previously to detect sphingolipid cleavage activity, we developed a method to search for novel sphingolipid cleavage activity in bacteria isolated from the soil on a restrictive carbon source. The methods we developed involved both growth of these isolates on Cer(1,3)P in growth medium over time and shorter incubations of the isolates with fluorescently-tagged SM and Cer(1,3)P. We additionally grew the isolates on agar plates containing our carbon source of interest.

Though the results from both the non-fluorescent assay with growth over time and the fluorescent incubation assay do not provide visible evidence for cleavage of Cer(1,3)P, NBD-SM, or NBD-Cer(1,3)P by the isolates, there could still be activity that these assays did not show. The substrate could have been degraded co-metabolically,⁴⁸⁻⁵⁰ and the energy that the cells obtain from the substrate on which they are grown may not be enough to support their robust growth.⁵¹⁻⁵³

In these assays, we did not see a change in lipid composition from before growth on Cer(1,3)P to after growth on Cer(1,3)P. Something we might have expected to see would be the disappearance of a Cer(1,3)P and a new appearance of SM on the TLC plate at the last time point. This would suggest that the bacterial isolates used Cer(1,3)P as a substrate and yielded SM as a product. However, we did not observe any change in lipid composition across time points. There may have been a change that we could not note by eye (i.e., the intensity of the lipids on the TLC plate may have decreased over time but may have been too faint for us to notice). Because of this

possibility, we would recommend quantifying the lipids on the TLC plates at the different time points with an imager, such as the Amersham Imager 600 (Cytiva).

Data from the protein assays in both growth over time on Cer(1,3)P and the fluorescent incubation showed an overall decreasing trend in protein concentration as the bacterial isolates were grown on Cer(1,3)P. The decreasing trend seen in these assays does not provide support for the isolates' ability to grow on and metabolize sphingolipids, as growth is typically indicated by an increase in protein concentration as cells are replicated and the carbon source is metabolized. Perhaps the isolates can obtain too little energy from Cer(1,3)P or SM that protein concentration may not be an accurate measure to assess their growth on these substrates. For example, the isolates may prefer to metabolize a carbon source like glucose but are still able to metabolize Cer(1,3)P or SM. Protein of the cells or proteins excreted may decrease overall as the isolates metabolize Cer(1,3)P, but the isolates could still be metabolizing these substrates.

Growth of isolate 6 on M9 agar plates containing Cer(1,3)P holds promise that at least this isolate can degrade Cer(1,3)P. There was no observed growth of isolate 6 on an M9 agar plate containing no carbon source, further supporting this point. Since we observed success of growth on solid medium and were not able to see that same success in our liquid cultures, biofilm formation and/or solid media may be necessary for these isolates to grow.⁵⁴ Lipids may be more accessible to the isolates in solid growth medium versus in liquid medium; these lipids are not very water soluble and may congregate in inaccessible vesicles in a liquid culture.

We think that it is strongly likely that we have bacterial isolates with a capacity to break down Cer(1,3)P because they were selected on multiple rounds of growth on a single carbon source and because when they were grown on petri dishes that are supplemented with Cer(1,3)P, colonies were visible while colonies were not visible on plates with no carbon source. However, the attempts so far to measure them in suspension culture and see activity based upon disappearance of added Cer(1,3)P or *in vitro* assays with NBD-Cer(1,3)P were unsuccessful. However, this may be a consequence of the less vibrant growth of the cells in suspension culture or that the enzyme was not properly induced by growth of the cells in medium that contained Cer(1,3)P.

In the future, spots on TLC plates can be quantified for fluorescence units by an imager; perhaps there is a change in the amount of substrate present that is not readily visible. The presence of a sphingolipid in the growth medium may be necessary for induction of sphingolipid metabolism. Though the assay with non-fluorescent Cer(1,3)P had Cer(1,3)P present in the growth medium, perhaps a higher quantity was needed, and there was no Cer(1,3)P present in the growth medium for cells that were incubated with NBD-Cer(1,3)P. There are many possibilities for modification of this procedure to assay and show the activity of bacterial isolates, such as to increase the concentration of Cer(1,3)P or to assay the growth of these isolates on solid medium.

CHAPTER 5: ISOLATED BACTERIA GENOMIC ANALYSIS

5.1 INTRODUCTION

To taxonomically identify the organisms that we isolated on SM and then Cer(1,3)P, we sequenced the isolate genomes and identified them taxonomically. We also searched for candidate protein-coding genes we anticipated finding in these isolates, namely ones that metabolize sphingolipids. It is important to mention that there is no known bacterial gene for metabolism of Cer(1,3)P; hence, the spider protein-coding reference genes used in the analysis are likely distantly related to their bacterial homologs, if any, which renders the bioinformatics analysis challenging.

5.2 MATERIALS AND METHODS

Preparation of Cells for Sequencing.

Isolates 4, 5, 6, and 7 were grown on M9+Cer(1,3)P agar plates from frozen glycerol stocks. Single colonies from these plates were used to inoculate M9+glucose media (isolates 4 and 5) and M9+Cer(1,3)P media (isolates 6 and 7). These cultures were grown overnight or longer for use in a DNA extraction kit.

DNA Extraction

DNA was extracted from isolates for genomic characterization using the Qiagen DNeasy Powersoil Prokit (#47014; Hilden, Germany).

DNA Concentration

To concentrate the DNA of samples, DNA was precipitated with ethanol according to the protocol described by Green and Sambrook (pp. 21-25).⁴⁶ Sodium acetate (3M, pH 5.2) was added to the DNA solutions at 1/10 of their volumes. Linear polyacrylamide (10-20 µg/mL) was added as a carrier molecule. After the addition of two volumes of ice-cold ethanol, samples were stored overnight at 4°C to allow the precipitate of DNA to form. DNA was recovered at maximum speed by centrifugation at 0°C for 15 minutes. The supernatant was removed, and the tube was filled halfway with ice-cold 70% ethanol. The sample was then centrifuged at maximum speed at 4°C for 2 minutes. The supernatant was removed, and the cap of the tube was left open for several hours so that the solvent could fully evaporate. The pellet was resuspended in TE buffer.

DNA Quantification

To quantify the DNA of samples, a NanoDrop Spectrophotometer (#ND-2000; Thermo Fischer Scientific; Waltham, MA) was first used. To more precisely quantify the DNA, a Qubit Assay (#Q33238; Thermo Fischer Scientific; Waltham, MA) for dsDNA was used.

Library Preparation and Sequencing

DNA sequencing libraries were prepared using the Illumina DNA Prep kit according to the manufacturer's instructions with an input of 24 ng of DNA. Libraries were amplified for 8 cycles and terminated after isolation of cleaned double stranded libraries. Library concentrations were determined by fluorescent quantification using a Qubit HS DNA kit and Qubit 2.0 fluorometer (ThermoFisher Scientific) and samples run on a High Sensitivity DNA chip using the Bioanalyzer 2100 instrument (Agilent) to determine library insert sizes. Libraries were sequenced for 300-cycles (2 x 150-bp paired-end) on an Illumina NextSeq 550 instrument (located in the School of Biological Sciences Molecular Evolution Core facility, Georgia Institute of Technology) as recommended by the manufacturer. This instrument carried out adapter trimming and demultiplexing of the sequenced samples.

Bioinformatic Analysis

This workflow is illustrated in Figure 11. Isolate raw reads were processed for quality control on Trimmomatic⁵⁵ and for assembly on SPAdes.⁵⁶ Assembled genomes were run on the TypeMat feature of the Microbial Genomes Atlas (MiGA)⁵⁷ for quality and taxonomic assignment. Prodigal⁵⁸ was used to predict where proteins are on the genome. To improve the genomes, any sequences that were shorter than 2 kilobase pairs (kb) were trimmed off, leaving predicted

proteins on the assembled sequences that were longer or equal (\geq) 2kb. These predicted proteins were passed to MicrobeAnnotator⁵⁹ for functional annotation prediction and clustering based on their metabolic similarity and completeness. MicrobeAnnotator created a heatmap visualization based on complete or incomplete modules in the Kyoto Encyclopedia of Genes and Genomes (KEGG) database⁶⁰ (Figure 17).

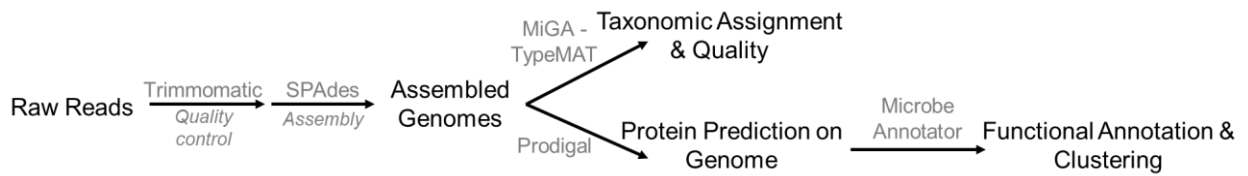


Figure 11. Workflow of the Bioinformatic Analysis of Isolate Genomes. Starting with raw reads we obtained from next-generation sequencing of the isolates, we ended with taxonomic assignment and functional annotation of the isolates.

5.3 RESULTS

Taxonomic Classification of Isolates

Using the TypeMat feature of the MiGA database,⁵⁷ isolates were taxonomically identified.

MiGA calculates the average nucleotide identities (ANI) and average amino-acid identity (AAI)

^{61,62} of a query genome, partial or complete, against all available genomes. Isolate 4 was assigned

to *Lentzea jiangxiensis* (p-value: 0.061, 96.27% ANI, 95.72% AAI) with a very high level of

completeness but only high level of quality (Figure 12 and Table 3) – due to a possible low level

of contamination. Isolate 5 was assigned to *Klebsiella variicola* (p-value: 0.017, 99.06% ANI,

99.30% AAI) with a very high level of completeness and excellent level of quality (Figure 13

and Table 3). Isolate 6 was assigned to *Klebsiella variicola* (p-value: 0.017, 99.04% ANI,

99.31% AAI) with a very high level of completeness and excellent level of quality (Figure 14

and Table 3). Isolate 7 was assigned to *Aeromonas media* (p-value: 0.11, 94.55% ANI, 95.41%

AAI) with a very high level of completeness and excellent level of quality (Figure 15 and Table

3). Since isolates 5 (99.06% ANI) and 6 (99.04% ANI) have >99% ANI, they are likely clones of

one another.

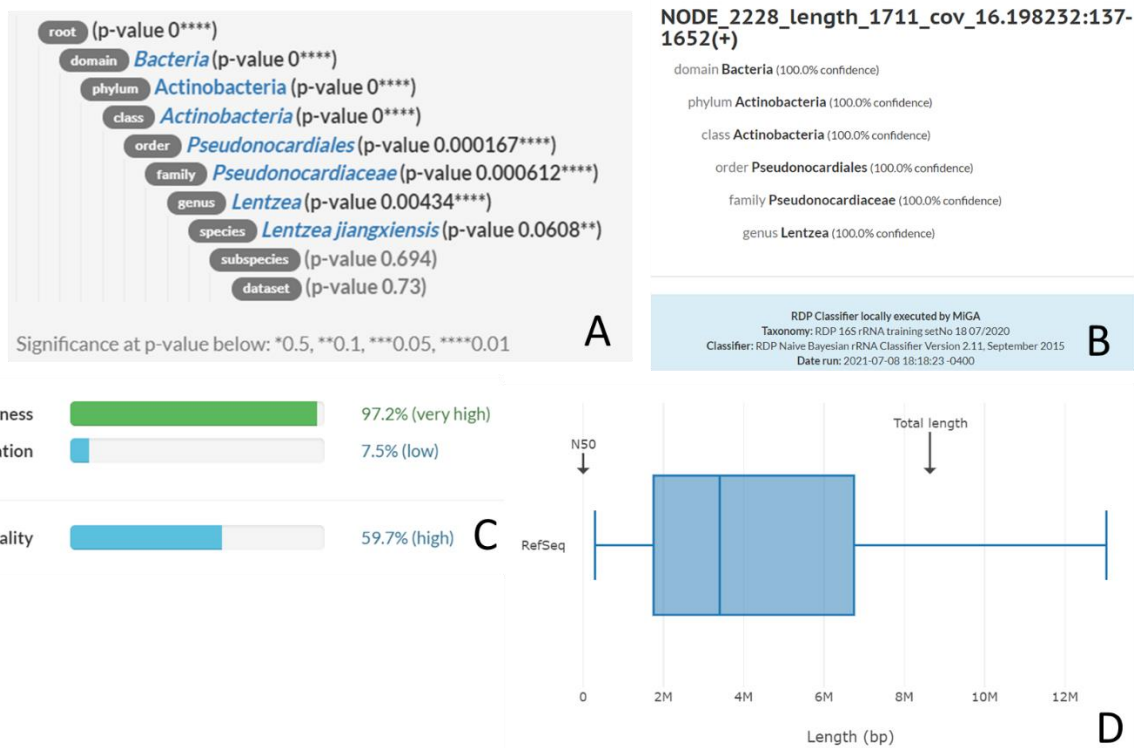


Figure 12. Isolate 4 Sequencing Quality and Classification Using the MiGA Webserver. (A) Taxonomic Classification and the Type-Material database (Type-Mat) of MiGA. (B) 16S rRNA gene sequence classification using the RDP Classifier. (C) Quality – Essential Genes. (D) Assembly.

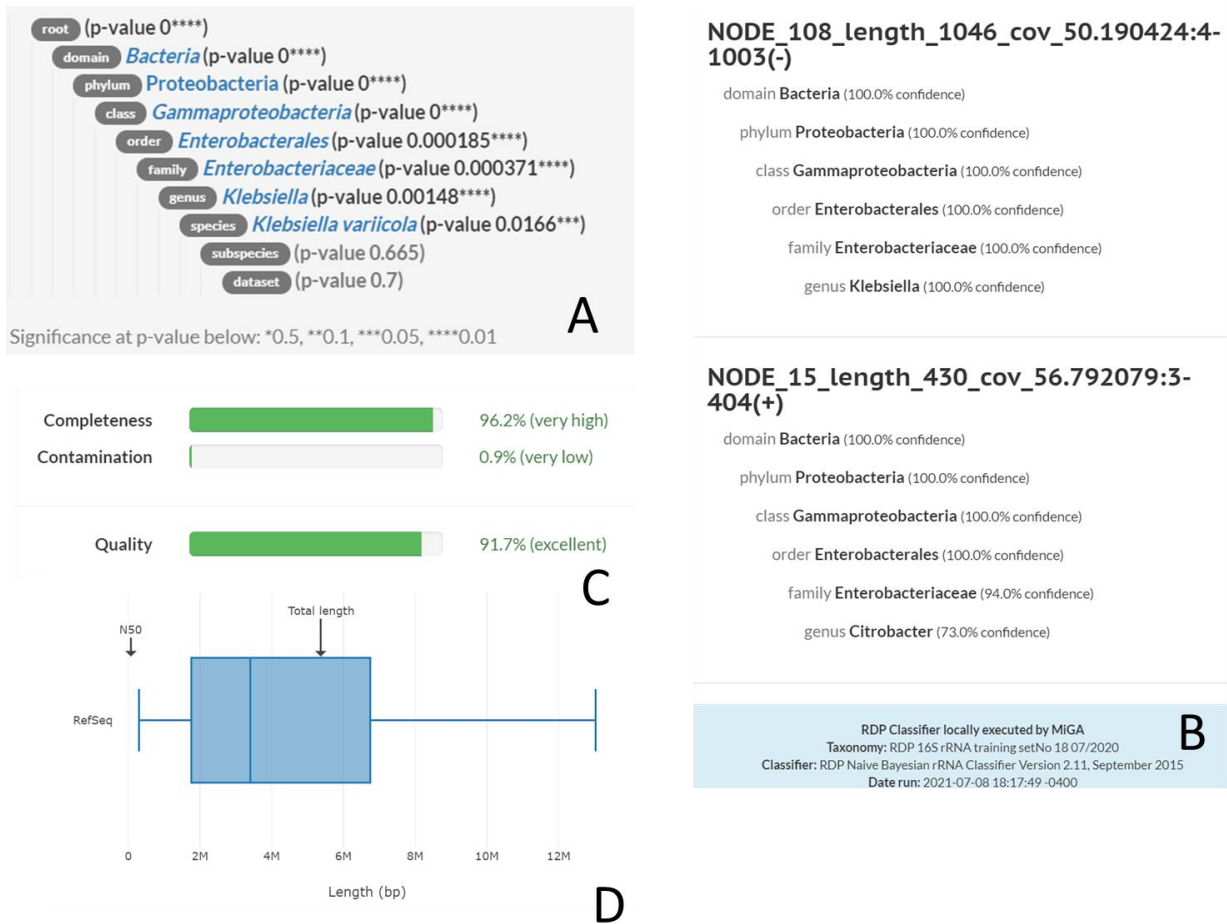


Figure 13. Isolate 5 Sequencing Quality and Classification Using the MiGA Webserver. (A) Taxonomic Classification and the Type-Material database (Type-Mat) of MiGA. **(B)** 16S rRNA gene sequence classification using the RDP Classifier. **(C)** Quality – Essential Genes. **(D)** Assembly.

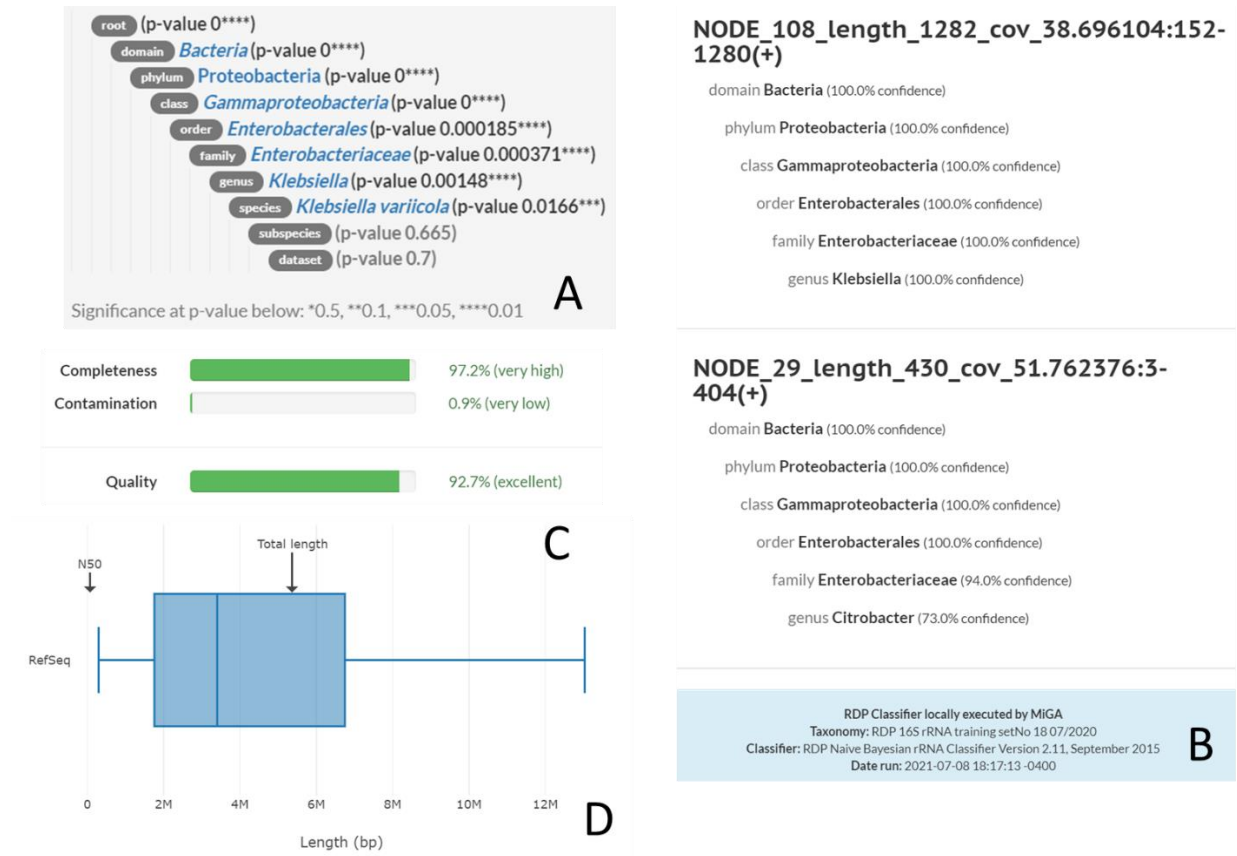


Figure 14. Isolate 6 Sequencing Quality and Classification Using the MiGA Webserver. (A) Taxonomic Classification and the Type-Material database (Type-Mat) of MiGA. **(B)** 16S rRNA gene sequence classification using the RDP Classifier. **(C)** Quality – Essential Genes. **(D)** Assembly.

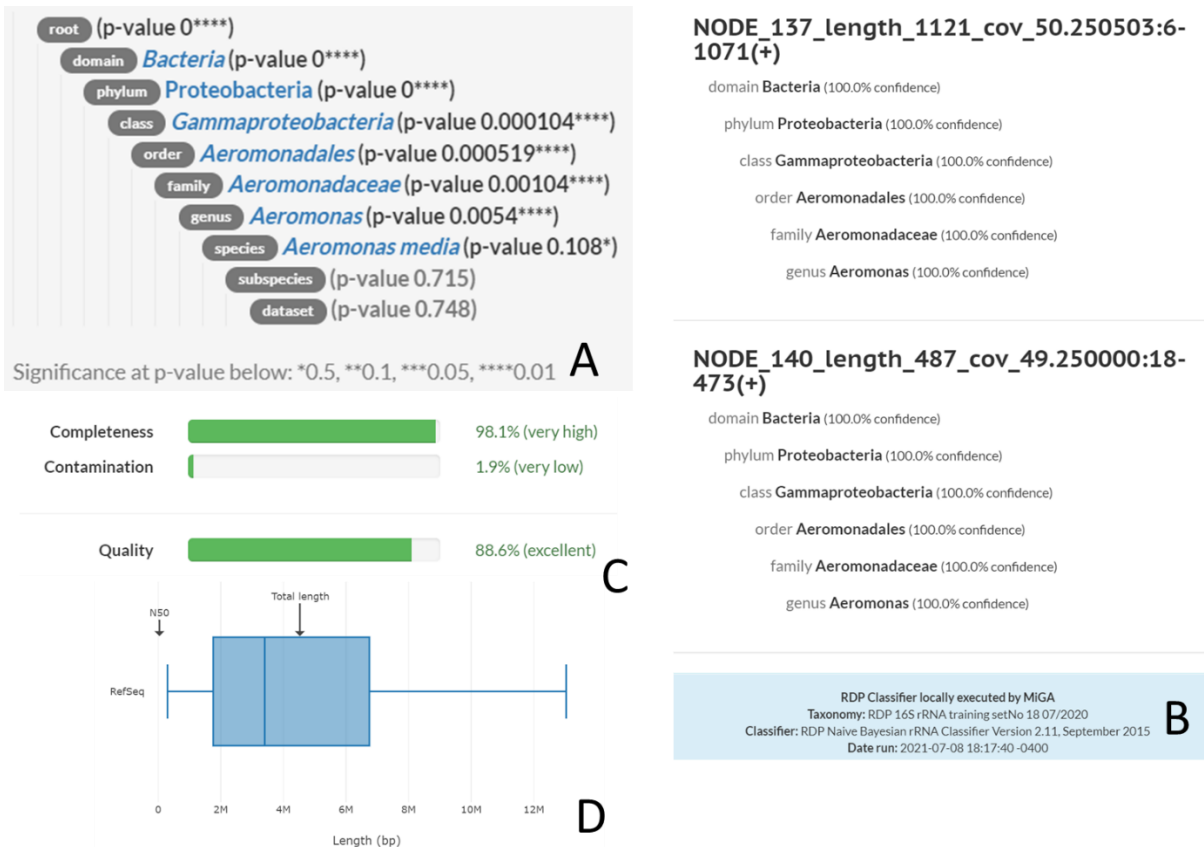


Figure 15. Isolate 7 Sequencing Quality and Classification Using the MiGA Webserver. (A) Taxonomic Classification and the Type-Material database (Type-Mat) of MiGA. **(B)** 16S rRNA gene sequence classification using the RDP Classifier. **(C)** Quality – Essential Genes. **(D)** Assembly.

Table 3. Summarized Information from the MiGA Webserver for Each Isolate.

		Isolate 4	Isolate 5	Isolate 6	Isolate 7
Taxonomic Classification	Closest Relative	<i>Lentzea jiangxiensis</i> GCA 900104175T (96.27%)	<i>Klebsiella varicola</i> NZ_CP072130T (99.06%)	<i>Klebsiella varicola</i> GCA 900978195T (99.04%)	<i>Aeromonas media</i> GCA 000819985T (94.55%)
	Genus	<i>Lentzea</i> (p-value: 0.0043)	<i>Klebsiella varicola</i> GCA 900978195T (99.05%)	<i>Klebsiella varicola</i> NZ_CP010523T (99.04%)	<i>Aeromonas</i> (p-value: 0.0054)
	Species	<i>Lentzea jiangxiensis</i> (p-value: 0.0051)	<i>Klebsiella varicola</i> (p-value: 0.017)	<i>Klebsiella varicola</i> (p-value: 0.017)	<i>Aeromonas media</i> (p-value: 0.11)
	Subspecies	NR (p-value: 0.00073)	NR (p-value: 0.0012)	NR (p-value: 0.0012)	NR (p-value: 0.00036)
Taxonomic Novelty	Species	NR (p-value: 0.035)	NR (p-value: 0.09)	NR (p-value: 0.09)	NR (p-value: 0.017)
	Location	NODE_2228_length_1711_cov_16.198232	NODE_108_length_1045_cov_50.190424	NODE_108_length_1282_cov_38.696104	NODE_137_length_1121_cov_50.250503
Ribosomal RNA (Small Subunit)	Contig (1)	138-1652 (+)	5-1003 (-)	153-1280 (+)	7-1071 (+)
	Product	16S ribosomal RNA	16S ribosomal RNA (partial), aligned only 63% of the 16S ribosomal RNA	16S ribosomal RNA (partial), aligned only 71% of the 16S ribosomal RNA	16S ribosomal RNA (partial), aligned only 67% of the 16S ribosomal RNA
	Contig (2)		NODE_15_length_430_cov_56.792079	NODE_29_length_430_cov_51.762376	NODE_140_length_487_cov_49.250000
	Location		4-804 (+)	4-804 (+)	19-473 (+)
	Product		16S ribosomal RNA (partial), aligned only 25% of the 16S ribosomal RNA	16S ribosomal RNA (partial), aligned only 25% of the 16S ribosomal RNA	16S ribosomal RNA (partial), aligned only 28% of the 16S ribosomal RNA
	Ssu	1	2	2	2
	Complete ssu	1	0	0	0
	Max Length	1,515	999	1,128	1,065
	Completeness	97.2%	96.2%	97.2%	98.1%
	Contamination	7.5%	0.9%	0.9%	1.9%
Quality (Essential Genes)	Quality	59.7%	91.7%	92.7%	88.6%
	Predicted Proteins	9,918	5,001	4,992	4,118
Gene Prediction	Average Length	261,1706 aa	314,8538 aa	315,374 aa	318,2987 aa
	Coding Density	89.9445%	88.0301%	88.0469%	86.8677%
	Codon Table	11	11	11	11
	Contigs	2,787	207	193	260
Assembly	N50	5,064 bp	73,517 bp	72,708 bp	40,532 bp
	Total Length	8,639,628 bp	5,266,066 bp	5,365,111 bp	4,525,724 bp
	Longest Sequence	30,136 bp	218,276 bp	190,822 bp	127,427 bp
	G+C Content	71.1099%	57.6089%	57.6151%	62.4273%
	X Content	0%	0%	0%	0%
	G-C Skew	-0.3289%	-1.1547%	-0.598%	-0.2943%
	A-T Skew	0.682%	0.2453%	-0.0923%	0.0406%

**NR = Not represented in database

Functional Annotation and Clustering of Genes

Gene functions were annotated based on predicted protein-coding genes in the genome (Figure 17). Isolate 4 had fairly high levels of completeness for protein-coding genes relating to lipid metabolism. In BLAST of the NCBI database, there was a relatively good alignment of the isolate 4 protein sequence X to a characterized SMase C (accession #P17627.1) in *Leptospira interrogans* (40.21% identity and 50% query cover) (Figure 16). Therefore, isolate 4 is a good candidate based upon this analysis for ability to degrade sphingolipids. Other isolates did not yield alignments to known sphingolipid-metabolizing genes for which we searched.

There were limitations in searching for predicted protein-coding genes of the isolates because the genes we were searching for (i.e., the ones that metabolize Cer(1,3)P) have not been characterized previously. We searched the predicted proteins of each isolate's genome for matches to candidate enzymes: SMase D (accession #AAW56831.1), a deacylase (accession #ACE14510.1), and a ceramidase (accession #CAC67511.1). There were no significant matches yielded from these searches.

```

Query 87 KILTHNVFLLPKTLPGWGNWQNERAQRIVSSNYIQNDVIVFDEAFDTDARKILLDGVR 146
+I T+NVF+L + L + NWGQ +RA + S+ + QDV+V +E FD A LL +R
Sbjct 6534 RIATYNVFMLSRNL--YPNWGQVQRADLVDSTGVLDGQDVVVLNEVFDNTASDRLLANLR 6361

Query 147 SEYPYQTDVIGRTKKGWDATLGLYRTDAFTNGGVVIVSKWPIEEKIQHVFKKGCADVF 206
YP+QT V+GR + GWD T G Y +GGV ++S+WPI +IQHV+++ GCGAD
Sbjct 6360 DTYPHQTPVLGRGRAGWDVTSGRYSDATPEDGGVAVLSRWPISTRIQHVVYRD-GCGADWL 6184

Query 207 SNKGFAYVRIDKNGRKFHIIIGTHVQAQDSGCANLGVSRVNFNEIRDFIDSKKIPKNEM 266
S KGFAYVR++ H+IGTH+QA+DS C + R Q EIR F+ ++ IP +E
Sbjct 6183 SAKGFAYVRVEAPAGPLHVIIGTHMQAEDSACTSAPGGYRAKQRAEIRAFLTARDIPASEP 6004

Query 267 VLIAGDLNVIKGSREYHQMLCILNVNPKYVGPFTWDTKTNEIAAFYKKEVPAY---- 322
V +AGDLNV S E+ +M+ L P+ G PF+WD N + Y P Y
Sbjct 6003 VYVAGDLNVAGASAEFPRMVADLGARTPEMGGHPFSWDCADNSVCRDQYG--PEYASEQ 5833

Query 323 LDYIFVSKSHFQPPIWQNLAYDPISAKTWT----AKGYTSDEFSDHYPVYG 369
LDY+ Q P+ +N + + W+ + YT ++ SDHYPV+
Sbjct 5832 LDYVLT----VQGPLLRNETRR-VKSPEWSIWSWGRKYTYNDLSDHYPVFA 5695

```

Figure 16. Alignment of Isolate 4 Genome to an SMase C. In BLAST of the NCBI database, the genome of isolate 4 (Sbjct) was aligned to the amino acid sequence encoding characterized SMase C (accession #P17627.1) in *Leptospira interrogans* (Query).

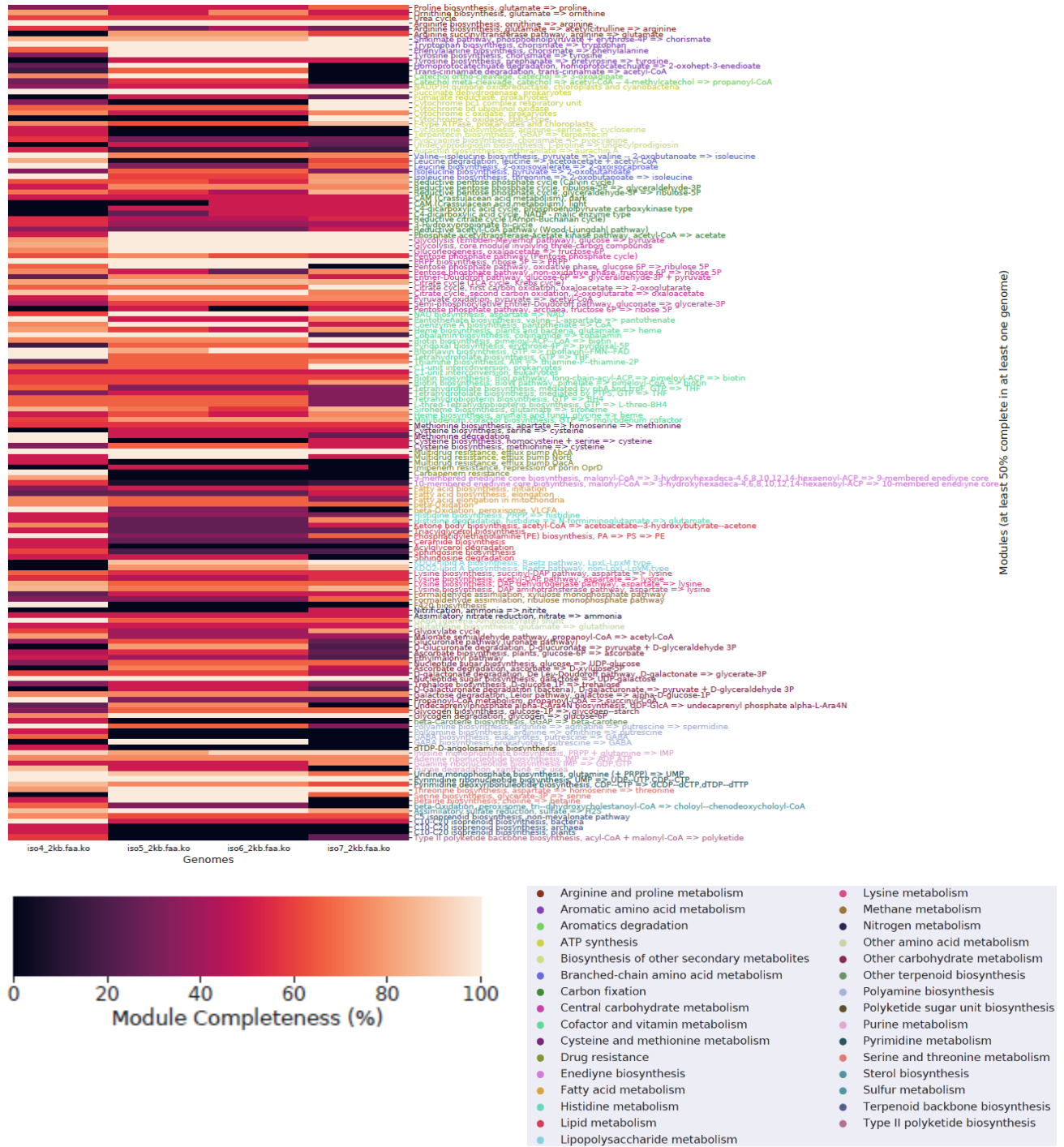


Figure 17. Heatmap Summary of Metabolic Modules Found on Each Isolate Genome. The colors correspond to various degrees of completeness (i.e., whether the isolate has all of the genes necessary for that metabolism).

5.4 DISCUSSION

K. variicola is an opportunistic pathogen and one causative agent of pneumonia,⁶³ and the two isolates that have been identified as *K. variicola*, 5 and 6, possess the same mucous-like phenotype as *K. variicola*.⁶⁴ Since *Lentzea jiangxiensis*, *Klebsiella variicola*, and *Aeromonas media* are presumed to metabolize the sphingolipid SM, further experimentation should be done to confirm their ability to degrade sphingolipids, and perhaps a novel enzymatic activity can be found. *Lentzea jiangxiensis* (isolate 4) had the highest level of completeness for predicted protein-coding genes that metabolize sphingolipids.

Since SMases C are almost universal in organisms that break down SM, the isolates would more likely have an SMase C than SMase D.^{65,66} Organisms that grew on SM likely had the SMase C. Therefore, the finding of a homologous SMase C in isolate 4 is not unexpected. Since there is no precedent for cleavage of Cer(1,3)P, there is not homolog that we know of for which to search.

In the future, we would recommend to look at gene expression levels in these isolates when grown on the substrate Cer(1,3)P versus when not grown on Cer(1,3)P (time-course transcriptomics). Such expression profiling could reveal genes that may be involved in Cer(1,3)P or other sphingolipid metabolism; such genes may be found among the hypothetical or poorly characterized genes in the genome given the lack of close reference homologs in the public databases.

CHAPTER 6: SUMMARY OF FINDINGS AND SUGGESTIONS FOR FUTURE STUDIES

Developing a solvent system and cocktail of standards allows for the fast and easy assessment of sphingolipid metabolic activity. The fluorescent substrates can be visualized immediately (i.e., there is no need to wait several hours for a plate to develop in an iodine tank to visualize the products). *L. reclusa* venom activity has been confirmed, and *K. hibernalis* activity has, for the first time, been shown to convert SM to Cer(1,3)P. The assay we have developed here could now be applied to *L. reclusa* and other spiders in the laboratory or even in a field (or clinical) setting.

Though the assays of the soil bacterial isolates did not show evidence for sphingolipid cleavage, there was evidence for sphingolipid utilization through their ability to grow on restrictive medium containing SM in their initial isolation and in the growth of isolates on agar plates containing Cer(1,3)P as a sole carbon source (whereas the isolates did not grow on agar plates that contained no carbon source). Therefore, it is likely that the conditions for assaying the enzyme(s) that are cleaving these substrates need further optimization for detection.

Since better growth was seen when the isolates were cultured on solid medium, this approach should be explored more in the future. Isolates may require biofilm formation for their growth, or the lipids may be more accessible to them in a solid medium versus in a suspension culture. Assaying the cells from agar plates directly is feasible, as these cells may more likely have sphingolipid cleavage activity than cells in a suspension culture would. Cells could be removed from the agar plates and used, or the agar on which the cells grow can be cut out, melted down, and assayed on TLC. If a fluorescent substrate is added directly to a TLC plate (rather than the

non-fluorescent ones that we added), metabolism of the substrate might be detected by the formation of fluorescent halos around the colonies on the plate.

Another alternative to the liquid cultures we have been using could be to dilute the enrichment culture as far as possible until activity can no longer be seen (the isolates may need to work together to degrade the substrate). A sequence analysis could then be done of this enrichment. Similarly, isolates could be grown on glucose and Cer(1,3)P/SM, and the concentration of glucose could gradually be decreased until the only carbon source that remains is a sphingolipid.

Two of the genomes of isolates 4, 5, 6, and 7 were taxonomically classified and revealed to be *K. variicola*. Isolate 4 showed the highest level of completeness for genes that metabolize lipids. Analyzing levels of expression (time-course transcriptomics) in the isolates growing on the substrate Cer(1,3)P versus not growing on Cer(1,3)P would help to identify the novel genes that we search for in Cer(1,3)P degradation.

Overall, a new activity in *K. hibernalis* is experimentally shown, and exploration into bacterial sphingolipid metabolism has been expanded. The TLC-based assay we have developed will make it easier to study sphingolipid metabolites and will aid in addressing related biological/biomedical questions.

REFERENCES

1. Thudichum JLW. *A Treatise on the Chemical Constitution of Brain*. London: Bailliere, Tindall, and Cox; 1884.
2. Kolter T, Proia RL, Sandhoff K. Combinatorial ganglioside biosynthesis. *J Biol Chem*. 2002;277(29):25859-25862. doi:10.1074/jbc.R200001200
3. Gault CR, Obeid LM, Hannun YA. *Sphingolipids as Signaling and Regulatory Molecules*. (Chalfant C, Del Poeta M, eds.). New York: Landes Bioscience and Springer Science+Business Media, LLC; 2010.
4. Tafesse FG, Ternes P, Holthuis JCM. The multigenic sphingomyelin synthase family. *J Biol Chem*. 2006;281(40):29421-29425. doi:10.1074/jbc.R600021200
5. Villani M, Subathra M, Im Y Bin, et al. Sphingomyelin synthases regulate production of diacylglycerol at the Golgi. *Biochem J*. 2008;414(1):31-41. doi:10.1042/BJ20071240
6. Kennedy EP. The Biosynthesis of Phospholipids. *Am J Clin Nutr*. 1958;6(3):216-220. doi:https://doi.org/10.1093/ajcn/6.3.216
7. Hanahan DJ, Chaikoff IL. The phosphorus-containing lipides of the carrot. *J Biol Chem*. 1947;168(1):233-240. doi:10.1016/s0021-9258(17)35110-4
8. Hanahan DJ, Chaikoff IL. A new phospholipide-splitting enzyme specific for the ester linkage between the nitrogenous base and the phosphoric acid grouping. *J Biol Chem*. 1947;169(3):699-705. doi:10.1016/s0021-9258(17)30887-6
9. Hanahan DJ, Chaikoff IL. On the nature of the phosphorus-containing lipides of cabbage leaves. *J Biol Chem*. 1948;172(1):191-198. doi:10.1016/S0021-9258(18)35628-X
10. Heller M. Phospholipase D. *Adv Lipid Res*. 1978;16:267-326. doi:10.1016/b978-0-12-024916-9.50011-1

11. Selvy PE, Lavieri RR, Lindsley CW, Brown HA. Phospholipase D - enzymology, functionality, and chemical modulation. *Chem Rev.* 2011;111(10):6064–6119.
doi:10.1021/cr200296t
12. Ponting CP, Kerr ID. A novel family of phospholipase D homologues that includes phospholipid synthases and putative endonucleases: Identification of duplicated repeats and potential active site residues. *Protein Sci.* 1996;5(5):914-922.
doi:10.1002/pro.5560050513
13. Koonin EV. A duplicated catalytic motif in a new superfamily of phosphohydrolases and phospholipid synthases that includes poxvirus envelope proteins. *Trends Biochem Sci.* 1996;21(7):242-243.
14. Zambonelli C, Roberts MF. Non-HKD Phospholipase D Enzymes: New Players in Phosphatidic Acid Signaling? *Prog Nucleic Acid Res Mol Biol.* 2005;79(04):133-181.
doi:10.1016/S0079-6603(04)79003-0
15. Zambonelli C, Casali M, Roberts MF. Mutagenesis of Putative Catalytic and Regulatory Residues of *Streptomyces chromofuscus* Phospholipase D Differentially Modifies Phosphatase and Phosphodiesterase Activities. *J Biol Chem.* 2003;278(52):52282-52289.
doi:10.1074/jbc.M310252200
16. Yang H, Roberts MF. Phosphohydrolase and transphosphatidylolation reactions of two *Streptomyces* phospholipase D enzymes: Covalent versus noncovalent catalysis. *Protein Sci.* 2003;12(9):2087-2098. doi:10.1110/ps.03192503
17. Hodgson ALM, Bird P, Nisbet IT. Cloning, nucleotide sequence, and expression in *Escherichia coli* of the phospholipase D gene from *Corynebacterium pseudotuberculosis*. *J Bacteriol.* 1990;172(3):1256-1261. doi:10.1128/jb.172.3.1256-1261.1990

18. Lucas EA, Billington SJ, Carlson P, McGee DJ, Jost BH. Phospholipase D promotes *Arcanobacterium haemolyticum* adhesion via lipid raft remodeling and host cell death following bacterial invasion. *BMC Microbiol.* 2010;10:270. doi:10.1186/1471-2180-10-270
19. Futrell JM. Loxoscelism. *Am J Med Sci.* 1992;304(4):261-267. doi:10.1097/00000441-199210000-00008
20. Tambourgi D V., Magnoli FC, Van Den Berg CW, et al. Sphingomyelinases in the venom of the spider *Loxosceles intermedia* are responsible for both dermonecrosis and complement-dependent hemolysis. *Biochem Biophys Res Commun.* 1998;251(1):366-373. doi:10.1006/bbrc.1998.9474
21. Tambourgi D V., Petricevich VL, Magnoli FC, Assaf SLMR, Jancar S, Dias Da Silva W. Endotoxemic-like shock induced by *Loxosceles* spider venoms: Pathological changes and putative cytokine mediators. *Toxicon.* 1998;36(2):391-403. doi:10.1016/S0041-0101(97)00063-9
22. Da Silva PH, Da Silveira RB, Helena Appel M, Mangili OC, Gremski W, Veiga SS. Brown spiders and loxoscelism. *Toxicon.* 2004;44(7):693-709. doi:10.1016/j.toxicon.2004.07.012
23. Tambourgi D V., Gonçalves-de-Andrade RM, van den Berg CW. Loxoscelism: From basic research to the proposal of new therapies. *Toxicon.* 2010;56(7):1113-1119. doi:10.1016/j.toxicon.2010.01.021
24. Lee S, Lynch KR. Brown recluse spider (*Loxosceles reclusa*) venom phospholipase D (PLD) generates lysophosphatidic acid (LPA). *Biochem J.* 2005;391(Pt 2):317-323. doi:10.1042/BJ20050043

25. Forrester LJ, Barrett JT, Campbell BJ. Red blood cell lysis induced by the venom of the brown recluse spider. The role of sphingomyelinase D. *Arch Biochem Biophys*. 1978;187(2):355-365. doi:10.1016/0003-9861(78)90046-2
26. Kurpiewski G, Forrester L, Barrett J, Campbell B. Platelet aggregation and sphingomyelinase D activity of a purified toxin from the venom of *Loxosceles reclusa*. *Biochim Biophys Acta*. 1981;678(3):467-476. doi:doi:10.1016/0304-4165(81)90128-8
27. Van Meeteren LA, Frederiks F, Giepmans BNG, et al. Spider and Bacterial Sphingomyelinases D Target Cellular Lysophosphatidic Acid Receptors by Hydrolyzing Lysophosphatidylcholine. *J Biol Chem*. 2004;279(12):10833-10836. doi:10.1074/jbc.C300563200
28. Dragulev B, Bao Y, Ramos-Cerrillo B, et al. Upregulation of IL-6, IL-8, CXCL1, and CXCL2 dominates gene expression in human fibroblast cells exposed to *Loxosceles reclusa* sphingomyelinase D: Insights into spider venom dermonecrosis. *J Invest Dermatol*. 2007;127(5):1264-1266. doi:10.1038/sj.jid.5700644
29. Lajoie DM, Zobel-Thropp PA, Kumirov VK, Bandarian V, Binford GJ, Cordes MHJ. Phospholipase D Toxins of Brown Spider Venom Convert Lysophosphatidylcholine and Sphingomyelin to Cyclic Phosphates. *PLoS One*. 2013;8(8):e72372. doi:10.1371/journal.pone.0072372
30. Stock RP, Brewer J, Wagner K, et al. Sphingomyelinase D activity in model membranes: structural effects of in situ generation of ceramide-1-phosphate. *PLoS One*. 2012;7(4):e36003. doi:10.1371/journal.pone.0036003
31. Tambourgi D V., De Sousa Da Silva M, Billington SJ, et al. Mechanism of induction of complement susceptibility of erythrocytes by spider and bacterial sphingomyelinases.

- Immunology*. 2002;107(1):93-101. doi:10.1046/j.1365-2567.2002.01483.x
32. van den Berg CW, Gonçalves-de-Andrade RM, Okamoto CK, Tambourgi D V. C5a receptor is cleaved by metalloproteases induced by sphingomyelinase D from *Loxosceles* spider venom. *Immunobiology*. 2012;217(9):935-941. doi:10.1016/j.imbio.2012.01.005
 33. Boudker O, Futerman AH. Detection and characterization of ceramide-1-phosphate phosphatase activity in rat liver plasma membrane. *J Biol Chem*. 1993;268(29):22150-22155.
 34. Gomez HF, Krywko DM, Stoecker W V. A new assay for the detection of *Loxosceles* species (brown recluse) spider venom. *Ann Emerg Med*. 2002;39(5):469-474. doi:10.1067/mem.2002.122914
 35. Arán-Sekul T, Rojas JM, Subiabre M, et al. Heterophilic antibodies in sera from individuals without loxoscelism cross-react with phospholipase D from the venom of *Loxosceles* and *Sicarius* spiders. *J Venom Anim Toxins Incl Trop Dis*. 2018;24(1):1-14. doi:10.1186/s40409-018-0155-x
 36. Ramos-Rodríguez HG, Valdez-Mondragón A, Méndez JD. Araneism by *Kukulcania* cf *tractans* in Mature Adult Male from Mexico: a Case Report. *World J Pharm Res*. 2019;8(3):120-129. doi:10.20959/wjpr20193-14296
 37. Teichgräber V, Ulrich M, Endlich N, et al. Ceramide accumulation mediates inflammation, cell death and infection susceptibility in cystic fibrosis. *Nat Med*. 2008;14(4):382-391. doi:10.1038/nm1748
 38. Wilderman PJ, Vasil AI, Johnson Z, Vasil ML. Genetic and biochemical analyses of a eukaryotic-like phospholipase D of *Pseudomonas aeruginosa* suggest horizontal acquisition and a role for persistence in a chronic pulmonary infection model. *Mol*

- Microbiol.* 2001;39(2):291-304. doi:10.1046/j.1365-2958.2001.02282.x
39. Driscoll JA, Brody SL, Kollef MH. The epidemiology, pathogenesis and treatment of *Pseudomonas aeruginosa* infections. *Drugs.* 2007;67(3):351-368. doi:10.2165/00003495-200767030-00003
 40. Williams BJ, Dehnbostel J, Blackwell TS. *Pseudomonas aeruginosa*: Host defence in lung diseases. *Respirology.* 2010;15(7):1037-1056. doi:10.1111/j.1440-1843.2010.01819.x
 41. Rolando M, Buchrieser C. A Comprehensive Review on the Manipulation of the Sphingolipid Pathway by Pathogenic Bacteria. *Front Cell Dev Biol.* 2019;7(August):1-8. doi:10.3389/fcell.2019.00168
 42. Futerman AH, Pagano RE. Use of N-([1-14C]Hexanoyl)-D-erythro-sphingolipids to Assay Sphingolipid Metabolism. *Methods Enzym.* 1992;209:437-446. doi:10.1016/0076-6879(92)09054-7
 43. Ladokhin AS, Isas JM, Haigler HT, White SH. Determining the membrane topology of proteins: Insertion pathway of a transmembrane helix of annexin 12. *Biochemistry.* 2002;41(46):13617-13626. doi:10.1021/bi0264418
 44. Kordahi T. Lipid-Protein Interactions via Fluorescence Quenching in Small Unilamellar Vesicles. *Honor Res Proj.* 2016;342.
 45. Lachmayr H, Merrill AH. Development of an Assay for Sphingomyelinase D Products in Venom from *Loxosceles reclusa* and Other Spiders. 2020. <https://smartechn.gatech.edu/handle/1853/63860>.
 46. Green M, Sambrook J. *Molecular Cloning: A Laboratory Manual.* 4th ed. Cold Spring Harbor: Cold Spring Harbor Laboratory Press; 2012.
 47. Geerlof A. M9 Mineral Medium. Helmholtz Center Munich. <https://www.helmholtz->

muenchen.de/fileadmin/PEPF/Protocols/M9-medium_150510.pdf. Published 2010.

Accessed August 17, 2020.

48. Li S, Wang S, Yan W. Biodegradation of methyl tert-butyl ether by co-metabolism with a pseudomonas sp. Strain. *Int J Environ Res Public Health*. 2016;13(9):1-10.
doi:10.3390/ijerph13090883
49. Vila J, Tauler M, Grifoll M. Bacterial PAH degradation in marine and terrestrial habitats. *Curr Opin Biotechnol*. 2015;33:95-102. doi:10.1016/j.copbio.2015.01.006
50. Meade JD, Hellou J, Patel TR. Aerobic co-metabolism of sulfur, nitrogen and oxygen heterocycles by three marine bacterial consortia. *J Basic Microbiol*. 2002;42(1):19-36.
doi:10.1002/1521-4028(200203)42:1<19::AID-JOBM19>3.0.CO;2-K
51. Yang M, Lu D, Yang J, et al. Carbon and nitrogen metabolic pathways and interaction of cold-resistant heterotrophic nitrifying bacteria under aerobic and anaerobic conditions. *Chemosphere*. 2019;234:162-170. doi:10.1016/j.chemosphere.2019.06.052
52. Mandel A, Zekker I, Jaagura M, Tenno T. Enhancement of anoxic phosphorus uptake of denitrifying phosphorus removal process by biomass adaption. *Int J Environ Sci Technol*. 2019;16(10):5965-5978. doi:10.1007/s13762-018-02194-2
53. Zhang Q, Tang D, Liu M, Ruan J. Integrated analyses of the transcriptome and metabolome of the leaves of albino tea cultivars reveal coordinated regulation of the carbon and nitrogen metabolism. *Sci Hortic (Amsterdam)*. 2018;231(September 2017):272-281. doi:10.1016/j.scienta.2017.11.026
54. Matsui H, Wagner VE, Hill DB, et al. A physical linkage between cystic fibrosis airway surface dehydration and Pseudomonas aeruginosa biofilms. *Proc Natl Acad Sci U S A*. 2006;103(48):18131-18136. doi:10.1073/pnas.0606428103

55. Bolger AM, Lohse M, Usadel B. Trimmomatic: A flexible trimmer for Illumina sequence data. *Bioinformatics*. 2014;30(15):2114-2120. doi:10.1093/bioinformatics/btu170
56. Bankevich A, Nurk S, Antipov D, et al. SPAdes: A new genome assembly algorithm and its applications to single-cell sequencing. *J Comput Biol*. 2012;19(5):455-477. doi:10.1089/cmb.2012.0021
57. Rodriguez-R LM, Gunturu S, Harvey WT, et al. The Microbial Genomes Atlas (MiGA) webserver: Taxonomic and gene diversity analysis of Archaea and Bacteria at the whole genome level. *Nucleic Acids Res*. 2018;46(W1):W282-W288. doi:10.1093/nar/gky467
58. Hyatt D, Chen GL, LoCascio PF, Land ML, Larimer FW, Hauser LJ. Prodigal: Prokaryotic gene recognition and translation initiation site identification. *BMC Bioinformatics*. 2010;11:119. doi:10.1186/1471-2105-11-119
59. Ruiz-Perez CA, Conrad RE, Konstantinidis KT. MicrobeAnnotator: a user-friendly, comprehensive functional annotation pipeline for microbial genomes. *BMC Bioinformatics*. 2021;22(1):1-16. doi:10.1186/s12859-020-03940-5
60. Kanehisa M, Goto S. KEGG: kyoto encyclopedia of genes and genomes. *Nucleic Acids Res*. 2000;28(1):27-30. doi:10.1093/nar/28.1.27
61. Konstantinidis KT, Tiedje JM. Genomic insights that advance the species definition for prokaryotes. *Proc Natl Acad Sci U S A*. 2005;102(7):2567-2572. doi:10.1073/pnas.0409727102
62. Caro-Quintero A, Konstantinidis KT. Bacterial species may exist, metagenomics reveal. *Environ Microbiol*. 2012;14(2):347-355. doi:10.1111/j.1462-2920.2011.02668.x
63. Long SW, Linson SE, Saavedra MO, et al. Whole-Genome Sequencing of Human Clinical *Klebsiella pneumoniae* Isolates Reveals Misidentification and Misunderstandings of

- Klebsiella pneumoniae, Klebsiella variicola, and Klebsiella quasipneumoniae. *mSphere*. 2017;2(4):e00290-17. doi:10.1128/mSphereDirect.00290-17
64. Rodríguez-Medina N, Martínez-Romero E, De la Cruz MA, et al. A Klebsiella variicola Plasmid Confers Hypermucoviscosity-Like Phenotype and Alters Capsule Production and Virulence. *Front Microbiol*. 2020;11(December):1-11. doi:10.3389/fmicb.2020.579612
65. Clarke CJ, Wu BX, Hannun YA. The neutral sphingomyelinase family: Identifying biochemical connections. *Adv Enzyme Regul*. 2011;51(1):51-58. doi:10.1016/j.advenzreg.2010.09.016
66. Clarke C, Snook C, Tani M, Matmati N, Marchesini N, Hannun Y. The extended family of neutral sphingomyelinases. *Biochemistry*. 2006;45(38):11247-11256. doi:doi:10.1021/bi061307z